

For Reference

NOT TO BE TAKEN FROM THIS ROOM

Ex libris
UNIVERSITATIS
ALBERTAEENSIS



THE UNIVERSITY OF ALBERTA

INVERSE MAGNETOTELLURIC ANALYSIS BY
THE METHOD OF SEQUENTIAL LAYERING

by



CHARLES EDWARD MOZESON

A THESIS

SUBMITTED TO THE FACULTY OF GRADUATE STUDIES AND RESEARCH IN
PARTIAL FULFILLMENT OF THE REQUIREMENTS FOR THE DEGREE OF
MASTER OF SCIENCE

Department of Physics
Edmonton, Alberta

Fall, 1971 -

Thesis
27 F
195

UNIVERSITY OF ALBERTA

FACULTY OF GRADUATE STUDIES AND RESEARCH

The undersigned certify that they have read, and recommend to the Faculty of Graduate Studies and Research for acceptance, a thesis entitled INVERSE MAGNETOTELLURIC ANALYSIS BY THE METHOD OF SEQUENTIAL LAYERING, submitted by Charles Edward Mozeson in partial fulfillment of the requirements for the degree of Master of Science.

ABSTRACT

Modifications and improvements to the Nabetani-Rankin method of sequential layer addition for a one-dimensional earth are presented and applied to several representative models to demonstrate the technique developed for inversion of magnetotelluric data. The inversion process was aided by the use of computer graphics and interactive programming. It was found that there are general rules to be followed for choosing layer parameters and once these methods are learned, the advantage and speed of interactive programming can be utilized. This method is inherently stable compared with the "least-squares" method of curve fitting.

ACKNOWLEDGEMENTS

I wish to express my sincere thanks to Dr. D. Rankin for suggesting and supervising this research problem and for his indefatigable assistance throughout this project.

I am grateful to Mr. S. Hoskin and Mr. N. Ouellette for their assistance in writing the computer programs; their support on this project has been invaluable.

Dr. I. K. Reddy is to be thanked for his advice and discussions, which helped forward the progress of this research.

I am indebted to Dr. W. J. Peeples for his friendly guidance during the beginning of my graduate work.

My sincere thanks go out to the many other people who have helped me in this research and who have forwarded my academic studies.

Throughout the course of this study, the author was financially supported by a Graduate Teaching Assistantship from the Department of Physics, University of Alberta.

Finally, I would like to acknowledge the contribution of Miss Laurie Soifer for her extreme patience and understanding during the last month of deadline pressure.

TABLE OF CONTENTS

| | Page |
|--|------|
| Chapter 1. INTRODUCTION | 1 |
| 1.1. Purpose of the Investigation | 1 |
| 1.2. Historical Review of the Magnetotelluric Method | 1 |
| 1.3. Existing Methods of Inverse Analysis | 3 |
| 1.4. Outline of Thesis | 9 |
| Chapter 2. MAGNETOTELLURIC THEORY | 10 |
| The Inverse Method | 18 |
| Chapter 3. THE METHOD OF SEQUENTIAL LAYER ADDITION | 26 |
| Chapter 4. RESULTS AND SUGGESTIONS FOR FURTHER WORK | 41 |
| REFERENCES | 50 |
| APPENDICES | 53 |
| A. Solution of the Wave Equation for a Source of Finite Dimensions | |
| B. Matrix Computation for Calculation of Surface Impedance | |
| C. Computer Programs | |

CHAPTER 1

INTRODUCTION

1.1. Purpose of the Investigation

The generalized magnetotelluric (MT) method consists of measuring the horizontal components of the naturally-occurring electromagnetic field variations at the surface of the earth and interpreting the sub-surface structure in terms of the apparent resistivity or the surface impedance. Direct interpretation of MT data, consisting of master-curve matching by trial and error, can be very tedious, especially if the number of parameters involved is large. Due to the availability of fast electronic computers and reliable recording equipment, the possibility exists of automatic inversion of MT data, which in turn may be a more reliable method and can save considerable computation time. Existing data inversion techniques have been based on "least-squares" methods of curve fitting, in which the mathematical and computational procedures tend to obscure the physical basis of the method and can lead to ambiguous or faulty results. The method of data inversion presented in this work makes use of the exact magnetotelluric expressions, which are intimately connected with the physical model and can thus match as closely as the measured data warrant.

1.2. Historical Review of the Magnetotelluric Method

Tikhonov (1950), Rikitake (1950, 1951) and Kato and

Kikuchi (1950) observed the existence of a correlation between the geomagnetic and telluric field variations at the surface of the earth, and suggested that it would be useful for depth sounding. The method did not become popular until Cagniard's definitive paper (1953), which presented a graphical technique for interpreting magnetotelluric field data under the assumption that the earth is horizontally stratified (that is, one-dimensional) and that the source fields are plane em waves. Wait (1954) and Price (1962) considered the problem of finite source dimensions and showed that Cagniard's results are valid only if the fields do not vary significantly over a horizontal distance of the order of a skin depth. However, Madden and Nelson (1964), considering realistic earth models, concluded that Cagniard's plane wave assumption is valid in most cases.

Magnetotelluric measurements have been made by many investigators (Cantwell, 1960; Srivistava et al., 1963; Vozoff et al., 1963; Tikhonov and Berdichevskii, 1966; Swift, 1967; Peeples, 1969; Reddy and Rankin, 1971; and others).

When the earth is anisotropic or inhomogeneous, the resistivity must be treated as a tensor quantity. Chetaev (1960), Cantwell (1960), Kovtun (1961), Bostick and Smith (1962), Swift (1967), Morrison et al. (1968) and others have shown how to compute the tensor components using spectral and statistical techniques.

The nature of the MT field for cylindrical inhomogeneities has been studied by several investigators, representative

works being those of Neves (1957), who studied the response of the MT field to dipping interfaces using finite difference techniques; d'Erceville and Kunetz (1962), who solved analytically for the vertical contact fault; and Rankin (1962), who solved analytically for the vertical dike.

Swift (1967), following the approach of Madden (1966), solved for two-dimensional problems by use of a transmission line analogy and used the method to study an electrical conductivity anomaly in the southwest United States.

There have been many recent attempts at inverting MT data (for example, Chetaev, 1966). The most common method is that of "least-squares" fitting of experimental curves (see Marquardt, 1963). Least-squares approaches have been adopted by Nelder and Mead (1964), Tikhonov (1965), Wu (1968), Patrick (1969), Patrick and Bostick (1969), Dmitriev (1970), Laird and Bostick (1970), and Word (1970).

In this work, the inversion technique of Nabetani and Rankin (1969) is used; the theoretical development and application follow in subsequent chapters.

1.3. Existing Methods of Inverse Analysis

Tikhonov (1965) showed the uniqueness of the solution of the inverse problem of MT sounding. That is, if the impedance which in general can be written

$$Z = Z(\rho; \omega) \tag{1.1}$$

or specifically

$$Z = Z(\omega) \quad (1.2)$$

$$\text{then } \rho = \rho(z) \quad (1.3)$$

is a unique dependance of resistivity ρ on depth z .

Thus,

$$Z(\omega) = A[\rho(z)] \quad (1.4)$$

where A is a nonlinear operator.

Inverse methods that have employed the "least-squares" technique involve the computation of either apparent resistivity or surface impedance. In this section, the theory of least-squares fitting will be developed briefly.

Letting ρ_{ci} be the calculated and ρ_{oi} be the observed apparent resistivity at period T_i , where the apparent resistivity is a function of ρ, z, T_i (which will be developed explicitly in Chapter 2), one computes the parameters that minimize the function

$$\Psi = \sum_i (\rho_{ci} - \rho_{oi})^2 \quad (1.5)$$

where

$$\Psi = \Psi(\rho_j, h_j) \quad (1.6)$$

with ρ_j, h_j being the resistivity and a thickness parameter associated with the j 'th value of ρ . Local minima occur where

$$\partial\Psi/\partial\lambda_j = 0, \quad j = 1, 2, \dots, 2n-1 \quad (1.7)$$

where λ_j is the j 'th parameter of Ψ . That is,

$$\lambda_1 = \rho_1, \dots, \lambda_n = \rho_n, \lambda_{n+1} = h_1, \dots, \lambda_{2n-1} = h_{n-1} \quad (1.8)$$

Writing

$$\rho_{ci} = f(\rho_1, \dots, \rho_n, h_1, \dots, h_{n-1}; T_i) = f(\lambda; T) \quad (1.9)$$

if f is linear in the λ 's and the λ 's are linearly-independent, the Ψ surfaces are ellipsoids:

$$\Psi = \frac{(\rho_1 - a_1)^2}{b_1^2} + \frac{(\rho_2 - a_2)^2}{b_2^2} + \dots + \frac{(h_{n-1} - a_{2n-1})^2}{b_{2n-1}^2} \quad (1.10)$$

If f is not linear, the surfaces are distorted; however, in the immediate vicinity of the minimum Ψ , the function $f(\lambda; T)$ behaves in a linear manner.

For a change in one of the parameters, there will be a corresponding change in ρ_{ci} . Consider the finite difference approximation

$$\begin{aligned} \partial \rho_{ci} / \partial \rho_j \approx \Delta \rho_{ci} / \Delta \rho_j = 1 / \Delta \rho_j \, f(\rho_1, \dots, \rho_{j-1}, \rho_j + \Delta \rho_j, \\ \rho_{j+1}, \dots, \rho_n, h_1, \dots, h_{n-1}; T_i) \end{aligned} \quad (1.11)$$

and similarly for changes in the h_j .

To first order,

$$d\rho_{ci} = (\rho_{oi} - \rho_{ci}) = \partial \rho_{ci} / \partial \rho_1 d\rho_1 + \dots + \partial \rho_{ci} / \partial h_n dh_n \quad (1.12)$$

and thus

$$\Psi = \sum_i (d\rho_{ci})^2 \quad (1.13)$$

Defining the matrices

$$D = (d\rho_1, \dots, dh_n) \quad (1.14)$$

$$P = \begin{vmatrix} \frac{\partial \rho_{c1}}{\partial \rho_1} & \dots & \frac{\partial \rho_{c1}}{\partial h_n} \\ \vdots & & \\ \frac{\partial \rho_{cn}}{\partial \rho_1} & & \frac{\partial \rho_{cn}}{\partial h_n} \end{vmatrix} \quad (1.15)$$

$$R = (\rho_{o1} - \rho_{c1}, \dots, \rho_{on} - \rho_{cn}) \quad (1.16)$$

One can then write (1.12) as

$$P^T P D = P^T R \quad (1.17)$$

And solving for D by inversion,

$$D = (P^T P)^{-1} P^T R \quad (1.18)$$

However, since ρ_{ci} is nonlinear in ρ and h , neglecting higher order derivatives in (1.12) may not lead to convergence if the norm of D is large. This can be seen by considering (1.17), in which a large value of D would require a small value of the norm of P. P is composed of terms resembling (1.11), which would itself be quite sensitive to changes in the values of its parameters, since its coefficients must of

necessity be very small. Thus, the operation (1.18) is unreliable and the process beset by inherent instability.

Most algorithms for least-squares estimation of nonlinear parameters have been based on either a Taylor series expansion of (1.9) or modifications of the method of steepest descent.

1.3.a Expansion of $f(\lambda; T)$ in a Taylor Series

In this method, corrections to the parameters are calculated on the assumption of local linearity of the function about the point $\lambda = \lambda_0 + \delta\lambda$:

$$f_i(\lambda_0 + \delta\lambda; T) = f_i(\lambda_0; T) + \sum_{j=1}^{2n-1} [\partial f_i / \partial \lambda_j] \delta\lambda_j + \dots \quad (1.19)$$

and truncating after the last linear term (since we assume that f is linear in λ and thus the higher derivatives are zero), (1.19) can be written

$$f = f_0 + P \, d\lambda \quad (1.20)$$

where f_0 is the original (uncorrected) function. Now $\delta\lambda$ appears linearly in (1.19) and (1.20) and can be found by setting

$$\partial \Psi / \partial (\delta\lambda_j) = 0 \quad (1.21)$$

for all j .

That is, by solving

$$A \, \delta\lambda = g \quad (1.22)$$

where

$$A = P^T P \quad (1.23)$$

$$P = \partial f_i / \partial \lambda_j \quad (1.24)$$

$$g = P^T (\rho_0 - f_0) \quad (1.25)$$

The corrections $\delta\lambda$ in each iteration must be small; otherwise the extrapolation may be beyond the region where f can be considered linear and the method may not lead to convergence. The conditions (1.21) lead to a stationary value of Ψ , which may not be a minimum for all parameters simultaneously. One most important requirement is a good "first guess" for the λ_j and even so, convergence is slow.

1.3.b. Another technique of solution is the modified Newton-Raphson method, where the second-order term in (1.19) is retained:

$$f_i(\lambda_0 + \delta\lambda; T_i) = f_i(\lambda_0; T) + \sum_j (\partial f_i / \partial \lambda_j) \delta\lambda_j + \frac{1}{2} \sum_{jk} \left(\frac{\partial^2 f_i}{\partial \lambda_j \partial \lambda_k} \right) \delta\lambda_j \delta\lambda_k \quad (1.26)$$

It has been found, though, that this method does not always decrease Ψ at each iteration. (See Laird and Bostick, P. 21.)

1.3.c. Gradient Methods

One moves in the direction of the negative gradient of Ψ (that is, in the direction of minimum Ψ). The step taken in each iteration is thus

$$\delta\lambda = - [\partial\Psi/\partial\lambda_1, \dots, \partial\Psi/\partial\lambda_{2n-1}]^T \quad (1.27)$$

The control of step direction and size is important here, for a bad choice could lead to divergence. Convergence in the neighbourhood of minimum Ψ is as a rule extremely slow.

Marquardt (1963) has devised a method for determination of step size and direction simultaneously, but uniqueness is not guaranteed. (See Wu, 1968.)

1.4. Outline of Thesis

In Chapter 2, the basic equations of the magnetotelluric field are derived and applied to a layered half-space. The Nabetani-Rankin inverse method is introduced and the relationships to be used in applying it are derived.

The method of sequential-layering and the theory behind the practical application are presented in Chapter 3.

In Chapter 4, computer graphics diagrams of curve matching by the method of sequential-layering are shown. Several representative earth models are presented to offer a feeling for the method. Chapter 4 is followed by conclusions and suggestions for further work, references and three Appendices.

CHAPTER 2

MAGNETOTELLURIC THEORY

In the em system of units, Maxwell's equations can be written

$$\nabla \times \vec{E} = -\partial \vec{H} / \partial t \quad (2.1)$$

$$\nabla \times \vec{H} = 4\pi \vec{J} + \partial \vec{D} / \partial t \quad (2.2)$$

$$\nabla \cdot \vec{E} = 4\pi d \quad (2.3)$$

$$\nabla \cdot \vec{H} = 0 \quad (2.4)$$

where \vec{J} is the electric current density and is related to the electric field by

$$\vec{J} = \sigma \vec{E} = \vec{E} / \rho \quad (2.5)$$

where σ is the electric conductivity, ρ the electric resistivity, and d the charge density of the medium. One can consider a single Fourier component of a general em disturbance, writing the time-dependent fields as

$$\begin{Bmatrix} E \\ H \end{Bmatrix} = \begin{Bmatrix} E_0 \\ H_0 \end{Bmatrix} e^{i\omega t} \quad (2.6)$$

In equation (2.2), applied to media such as the earth, displacement currents are negligible in comparison with conduction currents in the frequency range of interest ($\omega < 10^4 \frac{\text{Rad.}}{\text{Sec.}}$). Since we are considering media of finite conductivity, local concentrations of charge can also be neglected. Hence, the previous equations may be rewritten as:

$$\nabla \times \vec{E} = -\partial \vec{H} / \partial t \quad (2.7)$$

$$\nabla \times \vec{H} = 4\pi \vec{J} \quad (2.8)$$

$$\nabla \cdot \vec{E} = 0 \quad (2.9)$$

$$\nabla \cdot \vec{H} = 0 \quad (2.10)$$

To develop the MT equations, one solves Maxwell's equations subject to the following assumptions. Plane em waves impinge perpendicular to the surface of the earth and propagate vertically downward. This latter point is true for a non-zero angle of incidence, due to the relatively large refractive index of the earth with respect to the air for electromagnetic radiation. The co-ordinate system used is right-handed Cartesian with \hat{z} vertically downward and the x-y plane on the surface of the earth. Since we are not concerned with magnetic materials, we can consider the magnetic permeability to be approximately that of free space. That is, $\mu = \mu_0 = 1$.

Assuming the em fields polarized such that

$$\vec{E} = (E_x, 0, 0) \quad (2.11)$$

$$\vec{H} = (0, H_y, 0) \quad (2.12)$$

and making use of the vector identity

$$\nabla \times (\nabla \times \vec{E}) = \nabla (\nabla \cdot \vec{E}) - \nabla^2 \vec{E} \quad (2.13)$$

From (2.7) and (2.6),

$$\begin{aligned} \nabla \times \vec{E} &= -\partial \vec{H} / \partial t \\ &= -i\omega \vec{H} \end{aligned} \quad (2.14)$$

From (2.8) and (2.5),

$$\nabla \times \vec{H} = 4\pi\vec{J} = 4\pi\sigma\vec{E} \quad (2.15)$$

$$\begin{aligned} \nabla \times (\nabla \times \vec{E}) &= -i\omega (\nabla \times \vec{H}) \\ &= -4\pi\sigma i\omega\vec{E} \end{aligned} \quad (2.16)$$

Making use of (2.9), this equation can be written

$$\nabla^2 \vec{E} = 4\pi\sigma i\omega\vec{E} \quad (2.17)$$

with an identical equation for \vec{H} . The propagation equations for electromagnetic waves in the earth are thus

$$(\nabla^2 - k^2) \begin{Bmatrix} \vec{E} \\ \vec{H} \end{Bmatrix} = 0 \quad (2.18)$$

where $k^2 = 4\pi\sigma i\omega \quad (2.19)$

Solving equation (2.18), for example, for the electric field for the special case of an isotropic half-space, where the partial derivatives with respect to x and y are zero because of symmetry,

$$\nabla^2 \vec{E} = d^2\vec{E}_x/dz^2 \quad (2.20)$$

which has the general solution

$$E_x = Ae^{kz} + Be^{-kz} \quad (2.21)$$

The first term corresponds to an upward-travelling and the second term to a downward-travelling wave. In this particular case, there is no reflected (upward-travelling) wave;

indeed, for the em fields to remain finite for large values of z , the waves must decay with depth. Hence, $A = 0$. Therefore,

$$E_x = B e^{-kz} \quad (2.22)$$

and from (2.14)

$$\begin{aligned} H_y &= -\frac{1}{i\omega} \frac{dE_x}{dz} \\ &= \frac{k}{i\omega} B e^{-kz} = \frac{k}{i\omega} E_x \end{aligned} \quad (2.23)$$

One solves for ρ by using equation (2.19) and (2.23),

$$\rho = 2T \left| \frac{E_x}{H_y} \right|^2 \quad (2.24)$$

and the depth at which an electromagnetic Fourier component has diminished in magnitude to $1/e$ of its original value (known as the "skin depth")

$$\delta = \frac{1}{2\pi} (\rho T)^{1/2} \quad (2.25)$$

In the practical system of units, one measures the magnetic field in gammas, the electric field in millivolts/km., the period of wave oscillation in seconds, and the resistivity in ohm-metres.

$$\begin{aligned}
1 \text{ gamma} &= 10^{-5} \text{ em cgs.} \\
1 \text{ mv/km} &= 1 \text{ em cgs.} \\
1 \text{ km.} &= 10^5 \text{ em cgs.} \\
1 \text{ ohm-M} &= 10^{11} \text{ em cgs.}
\end{aligned}$$

In this system of units,

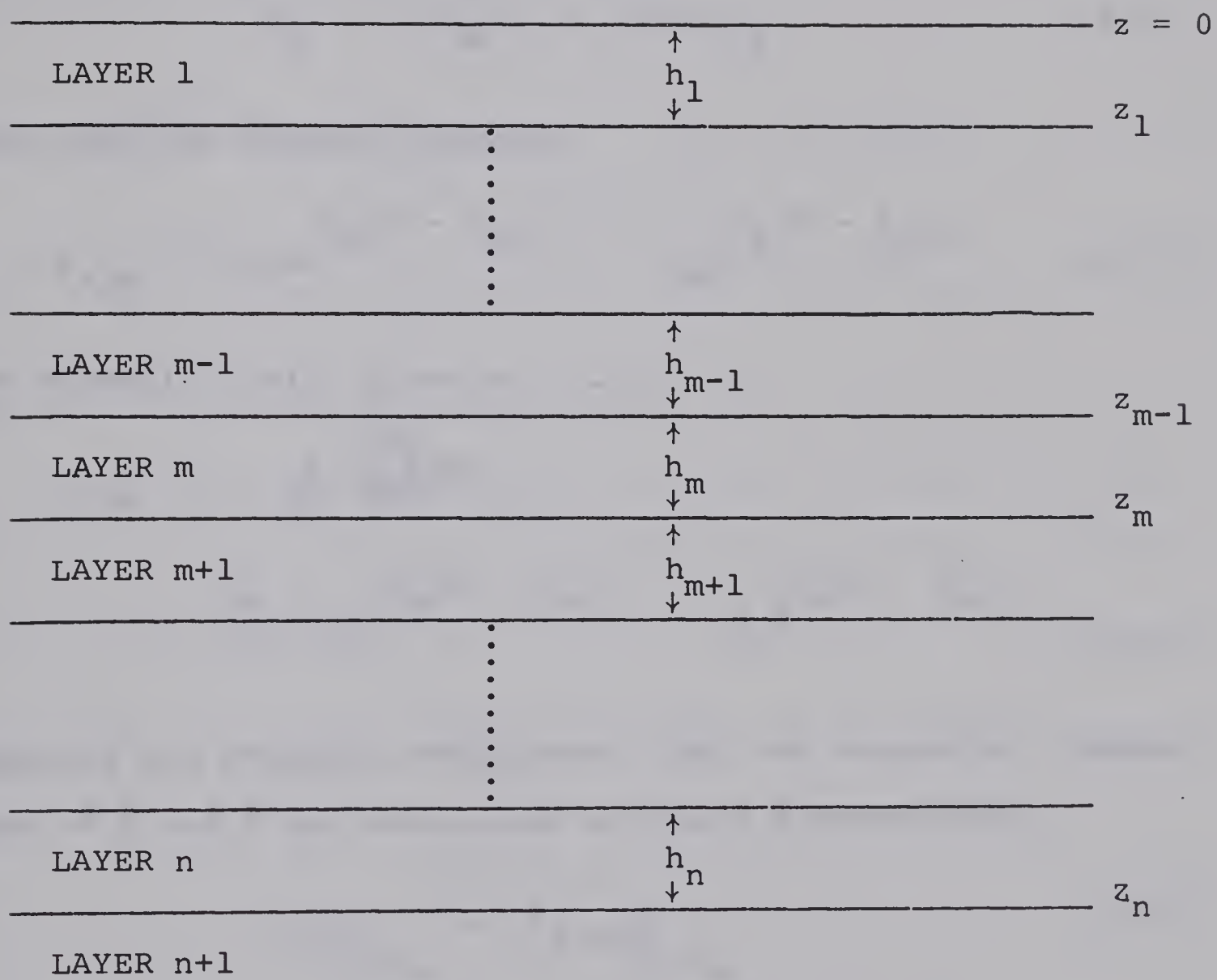
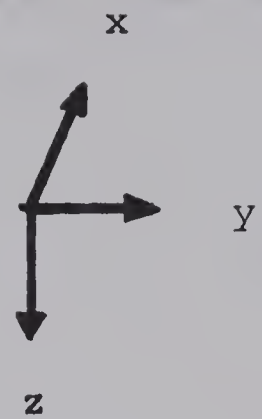
$$\rho = 0.2 T \left| \frac{E_x}{H_y} \right|^2 \quad (2.26)$$

$$\delta = \frac{1}{2\pi} (10 \rho T)^{1/2} \quad (2.27)$$

The case of a finite source (non-plane waves) has been dealt with by Wait (1954) and more completely by Price (1962). Price's analysis can be found in APPENDIX A. Madden and Nelson (1964) have shown, however, that the plane wave assumption is valid for the frequencies of interest in the MT method.

Cagniard (1953) developed relationships for the apparent resistivity in analogy to equation (2.26) for the case of two- and three-layer earth models and outlined a method for interpreting experimental results by matching with master curves. Master curves for 2,3,4, and 5-layer earth models have been computed by various authors (such as Yungul, 1961; Hasegawa, 1962; and Srivistava, 1967). However, the laborious algebraic work involved can be avoided by a simple iterative process for a general n-layered model using the digital computer directly. Adopting the co-ordinate system chosen earlier, so that the em fields are given by (2.11) and (2.12) and the notation for the earth cross-section in FIGURE 1, the

FIGURE 1: $n + 1$ layer earth model



wave equation for the electric field in the m 'th layer can be written (from 2.18)

$$\frac{d^2 E_{x,m}}{dz^2} = k_m^2 E_{x,m} \quad (2.28)$$

where

$$k_m^2 = 4\pi\sigma_m i\omega = 4\pi i\omega/\rho_m \quad (2.29)$$

which has the general solution

$$E_{x,m} = A_m e^{-k_m(z - z_{m-1})} + B_m e^{k_m(z - z_{m-1})} \quad (2.30)$$

The magnetic field, given by (2.14), is

$$\begin{aligned} H_{y,m} &= -\frac{1}{i\omega} \left(\frac{dE_{x,m}}{dz} \right) \\ &= \frac{k_m}{i\omega} \{ A_m e^{-k_m(z - z_{m-1})} - B_m e^{k_m(z - z_{m-1})} \} \end{aligned} \quad (2.31)$$

Applying the boundary conditions, that the tangential components of \vec{E} and \vec{H} are continuous across a discontinuity,

$$E_{x,m} \Big|_{z=z_m} = E_{x,m+1} \Big|_{z=z_m} \quad (2.32)$$

$$H_{y,m} \Big|_{z=z_m} = H_{y,m+1} \Big|_{z=z_m} \quad (2.33)$$

hence

$$A_m e^{-k_m h_m} + B_m e^{k_m h_m} = A_{m+1} + B_{m+1} \quad (2.34)$$

$$A_m e^{-k_m h_m} - B_m e^{k_m h_m} = \frac{k_{m+1}}{k_m} \{A_{m+1} - B_{m+1}\} \quad (2.35)$$

$$h_m = z_m - z_{m-1} \quad (2.36)$$

$$h_1 = z_1$$

Solving for the coefficients,

$$A_m = \frac{e^{k_m h_m}}{2k_m} \{ (k_m + k_{m+1}) A_{m+1} + (k_m - k_{m+1}) B_{m+1} \} \quad (2.37)$$

$$B_m = \frac{e^{-k_m h_m}}{2k_m} \{ (k_m + k_{m+1}) A_{m+1} + (k_m + k_{m+1}) B_{m+1} \} \quad (2.38)$$

For solutions to remain finite as $z \rightarrow \infty$, we demand that $B_{n+1} = 0$ in (2.30) (for the same reason as given following equation (2.21)). If one puts $A_{n+1} = 1$, since in any event it cancels out in the final ratios,

$$A_n = \frac{k_{n+1} + k_n}{2k_n} e^{k_n h_n} \quad (2.39)$$

$$B_n = \frac{k_n - k_{n+1}}{2k_n} e^{-k_n h_n} \quad (2.40)$$

At the surface of the earth,

$$E_x \Big|_{z=0} = A_1 + B_1 \quad (2.41)$$

$$H_Y \Big|_{z=0} = \frac{k}{i\omega} (A_1 - B_1) \quad (2.42)$$

In analogy with equation (2.26), one defines the apparent

resistivity ρ_a :

$$\rho_a = (0.2 \text{ T}) \left| \frac{E_x}{H_y} \right|_{z=0}^2 \quad (2.43)$$

and thus

$$\rho_a = (0.2 \text{ T}) \left| \frac{A_1 + B_1}{\frac{k}{i\omega} (A_1 - B_1)} \right|^2 \quad (2.44)$$

THE INVERSE METHOD

For our purposes, it is more convenient to deal with the intrinsic impedance

$$Z(\omega) = \frac{E_x}{i\omega H_y} \bigg|_{z=0} \quad (2.45)$$

which for an isotropic half-space from equation (2.23) can be written

$$Z(\omega) = \frac{1}{k} = \frac{1}{(4\pi\sigma i\omega)^{1/2}} \quad (2.46)$$

or

$$Z(T) = \frac{1}{2\pi} (\rho T/2)^{1/2} e^{-i\pi/4} \quad (2.47)$$

It should be noted in this expression that the electric field "leads" the magnetic field by a phase angle of $\pi/4$ radians. For a layered earth, one can write from (2.41) and (2.42),

FIGURE 2: The matrix equation (2.52)

[illegible]

$$Z(\omega) = \frac{A_0 + B_0}{k_0 (A_0 - B_0)} = \frac{A_1 + B_1}{k_1 (A_1 - B_1)} \quad (2.48)$$

since from (2.34) and (2.35) at the earth surface ($z=0$),

$$A_0 + B_0 = A_1 + B_1 \quad (2.49)$$

$$k_0 (A_0 - B_0) = k_1 (A_1 - B_1) \quad (2.50)$$

where k_0 is the propagation constant for free space ($k_0 = \omega/c$). The $(2n+2)$ equations (2.37), (2.38), (2.39), (2.40), (2.49), and (2.50) can be written in matrix notation

$$M^{-1}(x) = y \quad (2.51)$$

or (see APPENDIX B) as in (2.52), FIGURE 2. The solution of (2.51) is, by inversion,

$$x = M^{-1} (y) \quad (2.53)$$

By the use of determinants, one writes

$$x_1 = \frac{\det M_{11}}{\det M} y \quad (2.54)$$

where M_{11} is the appropriate cofactor. Or, from (2.52),

$$-(B_0/A_0) = \frac{\det M_{11}}{\det M} \quad (2.55)$$

Therefore,

$$\left. \frac{E_x}{i\omega H_y} \right|_{z=0} = \frac{1}{k_0} \frac{\det M - \det M_{11}}{\det M + \det M_{11}} \quad (2.56)$$

Because of the diagonal nature of the matrix M , the solution for the required determinants is simplified (See APPENDIX B). For example, for a 2-layered earth ($n=1$),

$$\left. \frac{E_x}{i\omega H_y} \right|_{z=0} = \frac{1}{k_1} \frac{1 + \kappa_1 e^{-2k_1 z_1}}{1 - \kappa_1 e^{-2k_1 z_1}} \quad (2.57)$$

where

$$\kappa_j = \frac{k_j - k_{j+1}}{k_j + k_{j+1}} \quad (2.58)$$

For a 3-layered earth ($n=2$),

$$\left. \frac{E_x}{i\omega H_y} \right|_{z=0} = \frac{1}{k_1} \frac{1 + \kappa_1 e^{-2k_1 z_1} + \kappa_2 e^{-2k_1 z_1 - 2k_2 (z_2 - z_1)} + \kappa_1 \kappa_2 e^{-2k_2 (z_2 - z_1)}}{1 - \kappa_1 e^{-2k_1 z_1} - \kappa_2 e^{-2k_1 z_1 - 2k_2 (z_2 - z_1)} + \kappa_1 \kappa_2 e^{-2k_2 (z_2 - z_1)}} \quad (2.59)$$

One can define

$$\Gamma_n = \frac{\det M - \det M_{11}}{\det M + \det M_{11}} = \frac{A_0 + B_0}{A_0 - B_0} \quad (2.60)$$

where

$$\Gamma_n = \frac{K_n^0 + K_n^1 + \dots + K_n^n}{K_n^0 - K_n^1 + \dots + (-1)^n K_n^n} = \frac{\sum_{i=0}^n [K_n^i]}{\sum_{i=0}^n [(-1)^i K_n^i]} \quad (2.61)$$

for an n -layered earth; and

$$K_n^0 = 1$$

$$K_n^1 = \sum_{p=1}^n \kappa_p \exp[-2 \sum_{i=1}^p k_i h_i]$$

$$K_n^2 = \sum_{p=1}^{n-1} \sum_{q=1}^n \kappa_p \kappa_q \exp[-2 \sum_{i=1}^q k_i h_i + 2 \sum_{m=1}^p k_m h_m]$$

.

.

.

$$K_n^m = \sum_{p_1=1}^{n+1-m} \sum_{p_2=p_1+1}^{n+2-m} \dots \sum_{p_m=p_{m-1}+1}^n \prod_{j=1}^m (\kappa_{p_j}) \prod_{i=1}^{m-1} (\exp[2(-1)^{m-1+i} \sum_{q_i=1}^{p_i} k_{q_i} h_{q_i}])$$

$$\times \exp[-2 \sum_{q_m=1}^{p_m} k_{q_m} h_{q_m}]$$

$$K_n^n = \prod_{j=1}^n (\kappa_j) \exp[-2 \sum_{i=1}^{n/2} (k_{2i} h_{2i})] \quad , \quad n \text{ even}$$

$$= \prod_{j=1}^n (\kappa_j) \exp[-2 \sum_{i=1}^{(n-1)/2} (k_{2i-1} h_{2i-1})] \quad , \quad n \text{ odd} \quad (2.62)$$

If one defines (See 2.58)

$$\kappa_j = \frac{\sqrt{\sigma_j} - \sqrt{\sigma_{j+1}}}{\sqrt{\sigma_j} + \sqrt{\sigma_{j+1}}} = \frac{\sqrt{\rho_{j+1}} - \sqrt{\rho_j}}{\sqrt{\rho_{j+1}} + \sqrt{\rho_j}} \quad (2.63)$$

and

$$H = 4\pi h_1 / \sqrt{\rho_1} \quad (2.64)$$

$$w_j = \sqrt{\rho_1 / \rho_j} h_j / h_1 \quad (2.65)$$

Then,

$$-2k_j h_j = -\sqrt{2i/T} H W_j \quad (2.66)$$

where

$$\sqrt{2i} = \sqrt{2} e^{i\pi/4} = 1 + i$$

Thus, if

$$Q = \sqrt{2i/T} H \quad (2.67)$$

then

$$-2k_j h_j = -Q W_j \quad (2.68)$$

Equation (2.62) then becomes

$$K_n^m = \sum_{p_1=1}^{n-m+1} \sum_{p_2=p_1+1}^{n-m+2} \dots \sum_{p_m=p_{m-1}+1}^n \prod_{j=1}^m (\kappa_{p_m})$$

$$\times \left\{ \prod_{\zeta=1}^{m-1} (\exp[2(-1)^{m+\zeta-1} \sum_{q_\zeta=1}^{p_\zeta} (W_{q_\zeta})]) \exp[-2 \sum_{q_m=1}^{p_m} (W_{q_m})] \right\}^Q$$

(2.69)

If we further define (and use 2.60)

$$V = \frac{1 - \Gamma_n}{1 + \Gamma_n} = \frac{1 - \frac{A_0 + B_0}{A_0 - B_0}}{1 + \frac{A_0 + B_0}{A_0 - B_0}} = - (B_0/A_0) \quad (2.70)$$

From (2.55)

$$V = \frac{\det M_{11}}{\det M} \quad (2.71)$$

From (2.70) and (2.61),

$$V = \frac{1 - \frac{\sum_{i=0}^n K_n^i}{\sum_{i=0}^n (-1)^i K_n^i}}{1 + \frac{\sum_{i=0}^n K_n^i}{\sum_{i=0}^n (-1)^i K_n^i}} = \frac{\sum_{i=0}^n [(-1)^i - 1] K_n^i}{\sum_{i=0}^n [(-1)^i + 1] K_n^i} \quad (2.72)$$

For $n=1$, a 2-layer earth (from 2.61 and 2.60),

$$\Gamma_1 = \frac{K_1^0 + K_1^1}{K_1^0 - K_1^1} = \frac{1 + K_1^1}{1 - K_1^1} \quad (2.73)$$

$$= \frac{1 + B_0/A_0}{1 - B_0/A_0} \quad (2.74)$$

Thus, from (2.70),

$$V = -B_0/A_0 = -K_1^1 = -\kappa_1 e^{-QW_1} \quad (2.75)$$

For $n=2$,

$$\Gamma_2 = \frac{1 + \frac{K_2^1}{1 - K_2^1} + \frac{K_2^2}{1 - K_2^2}}{1 - \frac{K_2^1}{1 - K_2^1} - \frac{K_2^2}{1 - K_2^2}} = \frac{1 + \frac{K_2^1}{1 + K_2^2}}{1 - \frac{K_2^1}{1 - K_2^2}} \quad (2.76)$$

so that from (2.70),

$$V = - \frac{K_2^1}{1 + K_2^2} \quad (2.77)$$

$$= - \frac{\kappa_1 e^{-QW_1} + \kappa_2 e^{-Q(W_1 + W_2)}}{1 + \kappa_1 \kappa_2 e^{-QW_2}} \quad (2.78)$$

and the "V-function" for any value of n can be obtained from (2.73) and (2.62). It can be regarded as the negative of the ratio of total reflected to total transmitted radiation at the surface of the earth ($z=0$). It should be noted that for $\sigma_2 < \sigma_1$, $k_2 \leq k_1$ and both A_0 and B_0 are greater than zero. Thus, $V = -B_0/A_0$ and the function will be negative. That is, it will behave like a curve of $-(\text{apparent resistivity})$. Thus for convenience, $-V$ will be plotted and the real part of the calculated values will be compared with the measured values.

CHAPTER 3

THE METHOD OF SEQUENTIAL LAYER ADDITION

In this method of inversion, a series of corrections is made, each of which modifies an already-computed curve. Thus, each correction corresponds to the result of interposing another layer above an original half-space, for which $V = 0$ and whose "exact" resistivity is obtained from well logs or DC resistivity measurements. This method has the advantage over the method of least-squares curve fitting in that one can observe the effect on the curve of modifying or adding layers and thus gain an intuitive feeling for the physical phenomena. In addition, this method does not suffer from the inherent instability and slow convergence rate of least-squares methods. Instead of approximating a curve by a polynomial, this method makes use of exact expressions.

Rearranging equation (2.72),

$$V K_n + K_n + V K_n + \dots + \left(\begin{matrix} V \\ 1 \end{matrix} \right) K_n^n = 0 \quad (3.1)$$

where

$$\left(\begin{matrix} V \\ 1 \end{matrix} \right) = \begin{matrix} V & \text{when } n \text{ is even} \\ 1 & \text{when } n \text{ is odd} \end{matrix}.$$

This can be expanded (with sign change, as explained in the last chapter):

$$\begin{aligned}
V = & \kappa_1 e^{-QW_1} + \kappa_2 e^{-Q(W_1+W_2)} + \kappa_3 e^{-Q(W_1+W_2+W_3)} \\
& + V_{\kappa_1 \kappa_2} e^{-QW_2} + V_{\kappa_1 \kappa_3} e^{-Q(W_2+W_3)} \\
& + V_{\kappa_2 \kappa_3} e^{-QW_3} \\
& + \kappa_1 \kappa_2 \kappa_3 e^{-Q(W_1+W_3)}
\end{aligned} \tag{3.2}$$

It can be seen that successive columns on the right side of (3.2) contain parameters of successively deeper layers; thus, the j 'th column does not contain the parameters of the $j+1$ 'th layer.

We now define the following sequence of approximations:

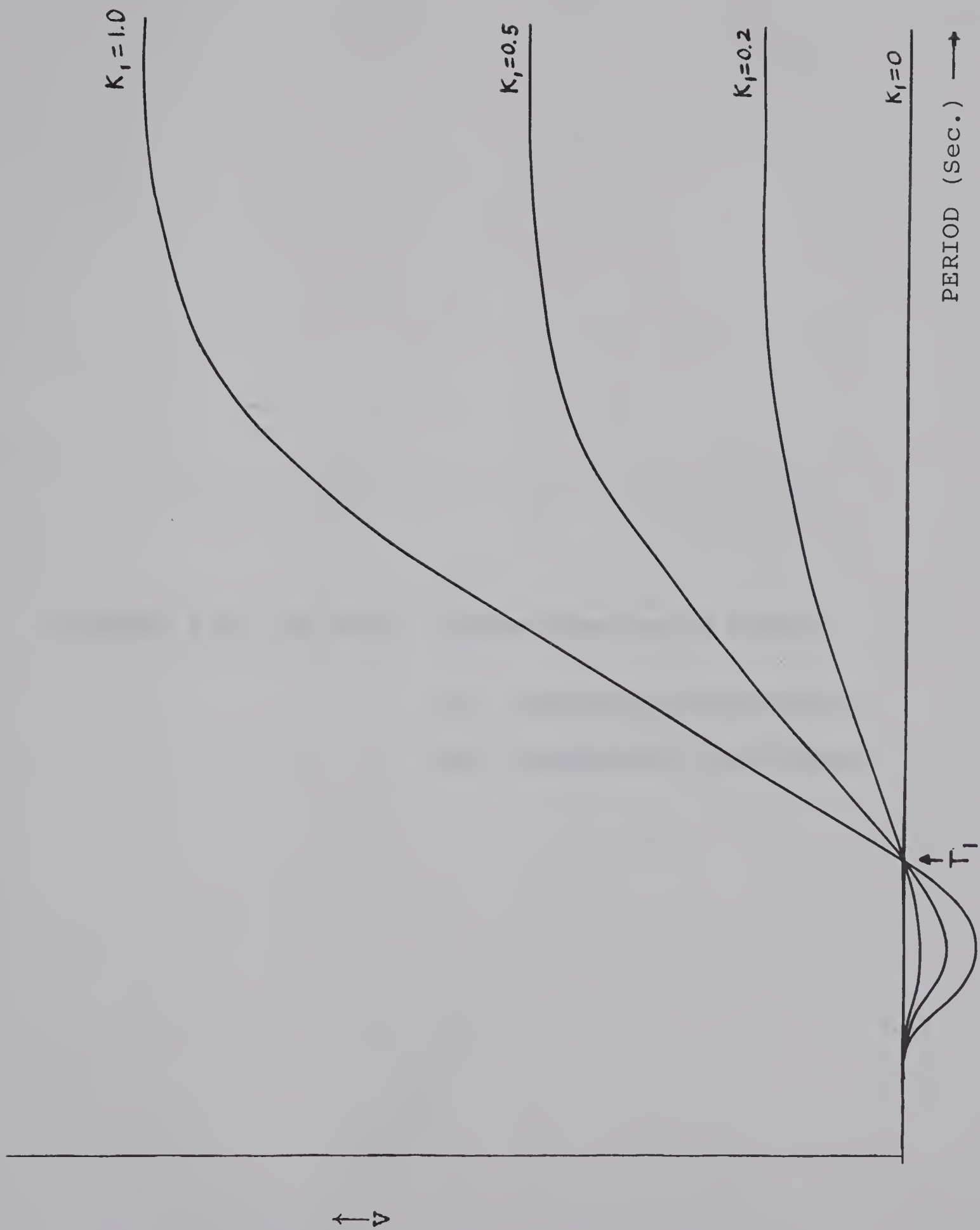
$$\begin{aligned}
V_1 &= \kappa_1 e^{-QW_1} & VC_1 &= V_1 \\
V_2 &= V_1 + \kappa_2 e^{-Q(W_1+W_2)} & VC_2 &= \frac{V_2}{1 + \kappa_1 \kappa_2 e^{-QW_2}} \\
V_3 &= V_2 + \kappa_3 e^{-Q(W_1+W_2+W_3)} & VC_3 &= \frac{V_3 + \kappa_1 \kappa_2 e^{-Q(W_1+W_3)}}{1 + \kappa_1 \kappa_2 e^{-QW_2} + \kappa_1 \kappa_3 e^{-Q(W_2+W_3)} + \kappa_2 \kappa_3 e^{-QW_3}} \\
& \cdot & & \\
& \cdot & & \\
& \cdot & &
\end{aligned} \tag{3.3}$$

The VC_j can be seen to be the exact expressions for a $(j+1)$ -layered earth (Compare with the expressions 2.75 and 2.78).

Consider the residuals defined as follows:

$$\begin{aligned}
R_1 &= VC_1 - V \\
R_2 &= VC_2 - V \\
R_3 &= VC_3 - V
\end{aligned} \tag{3.4}$$

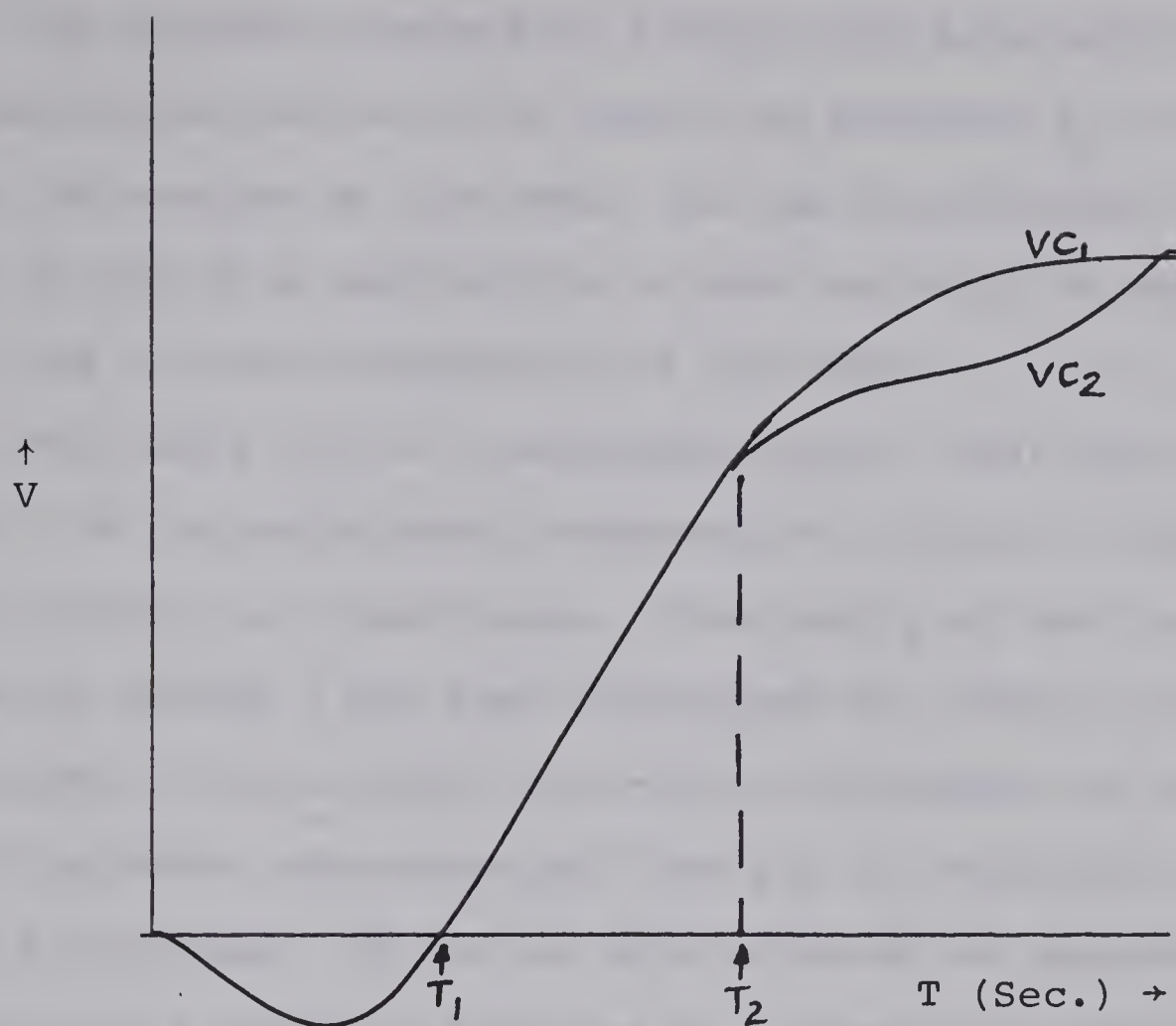
FIGURE 3: A family of two-layer curves



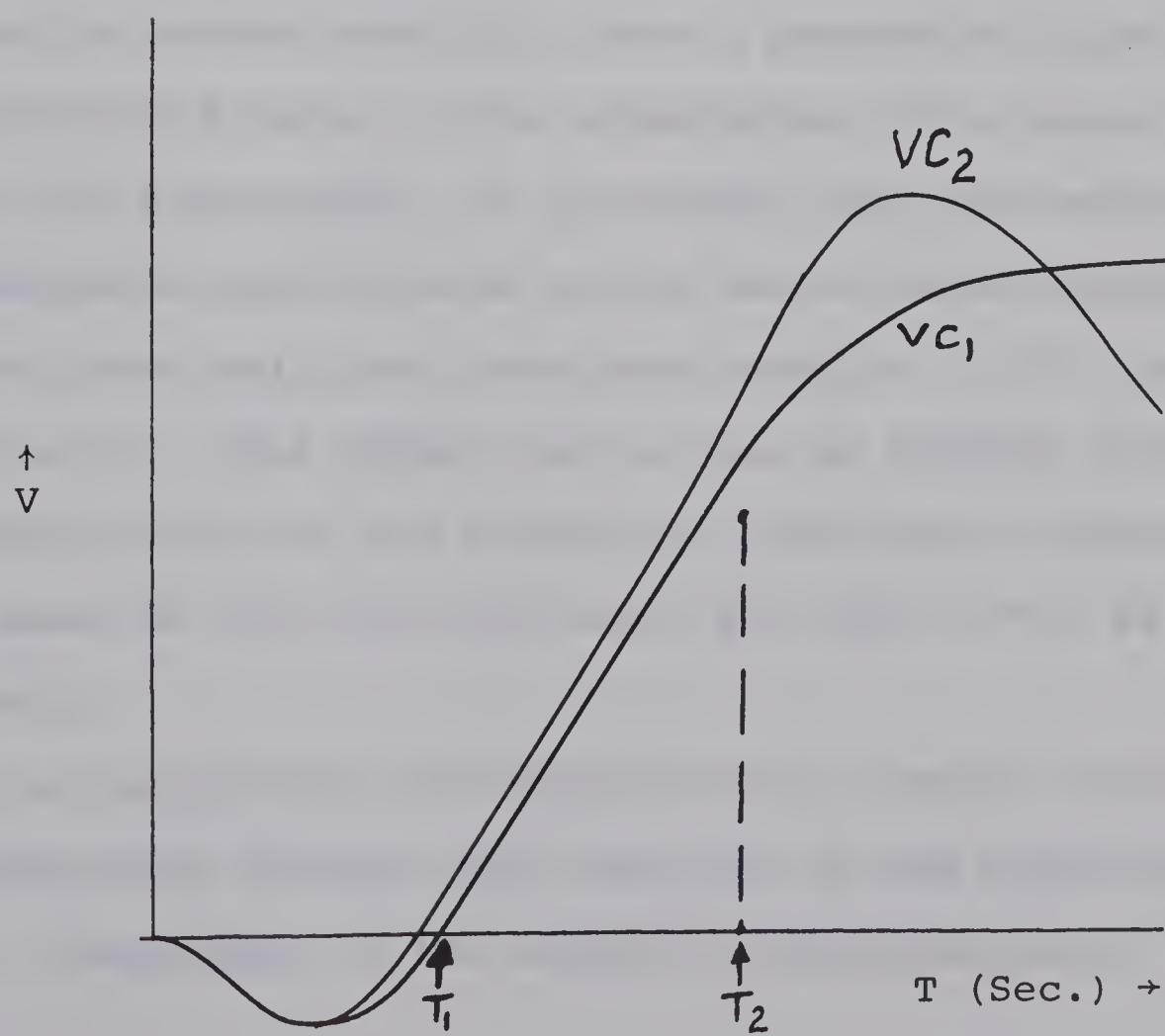
FIGURES 4(a) and 4(b): Three-layer earth models

(a) resistive half-space

(b) conductive half-space



4 (a)



4 (b)

The process consists of fitting the data with successively calculated curves of VC until the residual R_n is smaller than the scatter in the data. In the calculations, the real part of the VC's and the R's is used and will be compared with the in-phase components of the data.

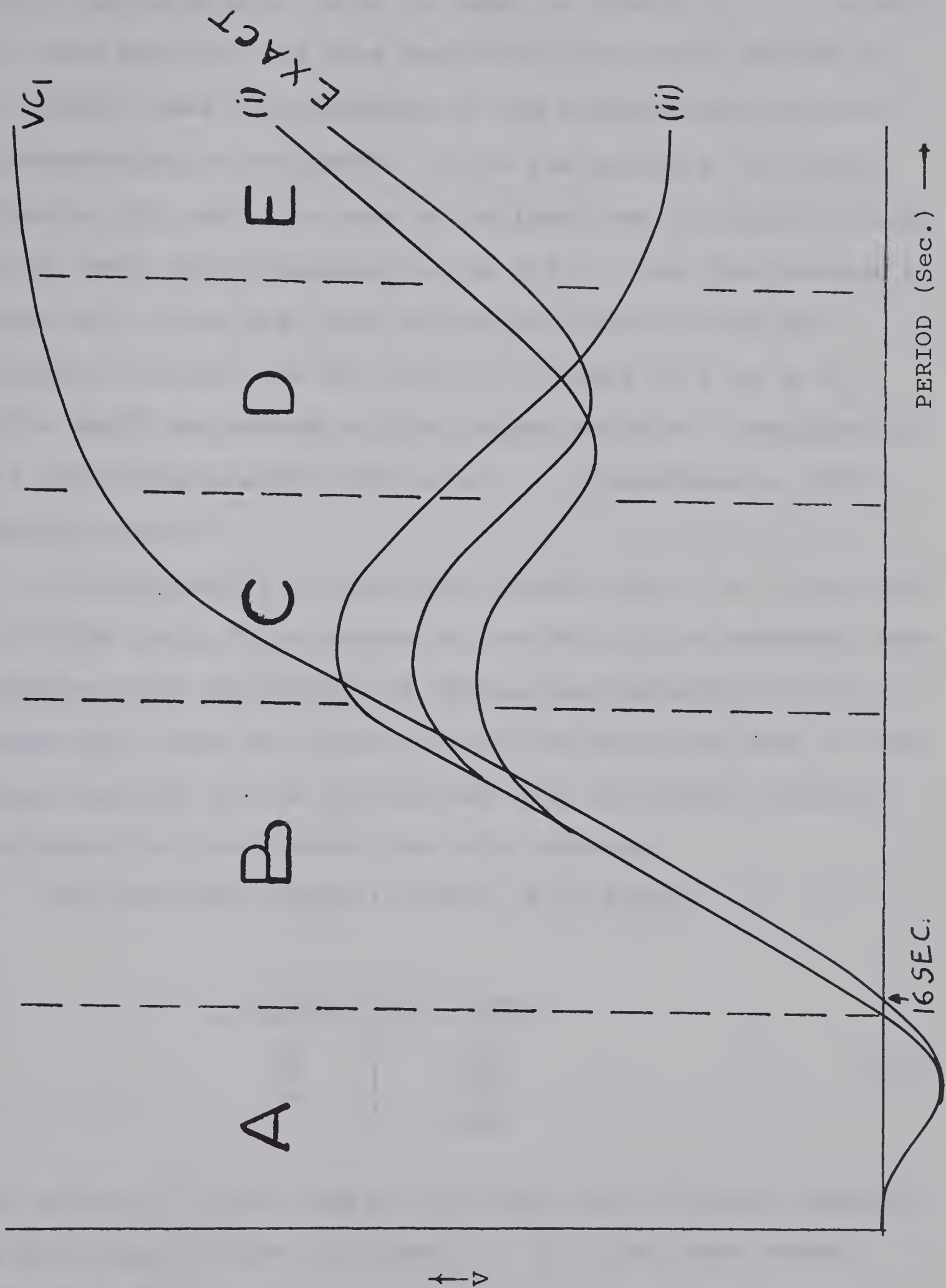
The curve VC_1 is a two-layer curve-- that is, the function V for an earth model composed of a layer of finite thickness resting on a half-space. The family of two-layer curves shown in FIGURE 3 has been calculated for various resistivity contrasts. For a given first-layer thickness and resistivity, the "rightmost zero-crossing" for all of the curves (called T_1) is the same. If one is able to match an experimental curve with a curve of the type VC_1 , then the substructure can be interpreted unambiguously as two-layered. If the curve cannot be matched with VC_1 , then a successive approximation is calculated based on the introduction of a second layer above the half-space. It is obvious that the reflection and transmission coefficients at the second layer boundary will change drastically and thus from equation (2.70), so will the function V. This effect can be seen in FIGURES 4(a) and 4(b), in which resistive and conductive half-spaces respectively are added to the two-layer model for which $\kappa=0.5$ as shown in FIGURE 3.

In the process of interpretation, certain factors must be taken into account which are part of the physical phenomenon, independent of the method of interpretation. Since the

earth is a resistive medium, there exists a skin depth, as defined in equation (2.25), which is the layer thickness at which the amplitude has decreased to $1/e$ of its value at the upper boundary. It follows from the form of the equation that for shorter periods, there is a correspondingly smaller depth to which the em wave can probe; or conversely, the effect of resistivity changes at depth can have little effect on the shorter period values of either V , ρ , or Z . Thus, in calculating the first approximation to V , it is essential that the curve match for the shorter periods and that the departure from the observed values be in such a direction that the next approximation causes the curve to match for successively longer periods without departing significantly from the good match already obtained at the shortest periods. One is assisted in this process by the shielding effect already discussed. However, there is the corresponding problem that it requires thicker layers and higher resistivity contrasts in order to be observable for successively deeper layers, which also implies longer periods. In all methods, thin layers and/or low resistivity contrasts which lie at depth are invisible and tend to be averaged with their neighbours. In the choice of parameters, it is essential to anticipate the effect that the deeper layers will have, not only on the curve for longer but also in the shorter period region.

FIGURES (4a) and (4b) illustrate the effect of adding an additional layer to the two-layer model with $\kappa = 0.5$, for

FIGURE 5: Curve fitting for model (3.5)



which the calculated curve is shown in FIGURE (3). It should be noted that for the more resistive substratum (FIGURE 4a), the effect does not propagate to the shorter periods and the zero-crossing is unaltered. It is the period at the zero-crossing, T_1 , which is used to estimate the thickness of the first layer (See equations 3.6 to 3.8.). One then chooses a value of κ_1 that will give values of V which match the straight line part of the curve for values of T up to T_2 , which would correspond to the largest value of T employed if the earth consisted of two layers. κ_1 determines ρ_2 from equation (2.63).

In the case of a conducting second layer, as illustrated in FIGURE (4b), T_1 is chosen to the left of the observed zero crossing since the effect of adding the conducting third layer will cause the curve not only to be pulled down at the longer periods but to be affected also at shorter periods, including the range about the zero crossing.

For the model shown in table (3.5) below,

| h (km) | R (Ω -M) | (3.5) |
|----------|--------------------|-------|
| 5 | 10 | |
| 30 | 1000 | |
| 30 | 50 | |
| | 4000 | |

for which $\kappa_1 = 0.818$ and $\kappa_2 = -0.635$, the V function appears as the "exact" curve of FIGURE 5. If T_1 had been chosen correctly (h_1 correct) but

κ_1 too large
too small, then R_1 would have been $\begin{matrix} < \\ > \end{matrix}$ 0 in region A.

If h_1 , h_2 , and κ_2 were correct, but

κ_1 too large
too small, then R_2 would have been $\begin{matrix} > \\ < \end{matrix}$ 0 in region C.

If h_1 , κ_1 , and κ_2 were correct but h_2 too small, the second approximation curve would resemble (i); if too large, it would resemble (ii).

These considerations apply to successive approximations. If the parameters chosen in the j 'th approximation (that is, h_j , κ_j) are not correct, then the $(j+1)$ 'th approximation will show the error.

The actual determination of h_1 is made as follows; The zero-crossing corresponding to a two-layer earth is the point at which

$$VC_1 = \kappa_1 e^{-QW_1} = 0 \quad (3.6)$$

From equations (2.64) to (2.68), one can write the real part:

$$\kappa_1 e^{-H/\sqrt{T_1}} \cos \frac{H}{\sqrt{T_1}} = 0$$

from which

$$\frac{4\pi h_1}{\sqrt{10} \rho_1 T_1} = (2n + 1) \frac{\pi}{2}, \quad n = 0, 1, 2, \dots \quad (3.7)$$

For the rightmost zero crossing, $n = 0$ and

$$h_1 = \sqrt{.10 \rho_1 T_1} / 8 \quad (3.8)$$

which is identical to the result of Cagniard for the two-layer apparent resistivity curves.

Analysis of curve shifts due to this technique is aided by residual analysis. The curve shift from VC_1 to VC_2 is:

$$\text{REAL}(VC_2 - VC_1) = \text{REAL} \left[\frac{\kappa_1 e^{-QW_1} + \kappa_2 e^{-Q(W_1+W_2)}}{1 + \kappa_1 \kappa_2 e^{-QW_2}} - \kappa_1 e^{-QW_1} \right] \quad (3.9)$$

$$= \text{REAL} \left[\frac{\kappa_2 (1 - \kappa_1^2) e^{-Q(W_1 + W_2)}}{1 + \kappa_1 \kappa_2 e^{-QW_2}} \right] \quad (3.10)$$

$$= \frac{\kappa_2 (1 - \kappa_1^2) e^{a+b} \{ \kappa_1 \kappa_2 e^b \cos(a) + \cos(a+b) \}}{1 + 2\kappa_1 \kappa_2 e^b \cos(b) + (\kappa_1 \kappa_2 e^b)^2} \quad (3.11)$$

where we define

$$\begin{aligned} a &\equiv -4\pi h_1 / \sqrt{.10 \rho_1 T} \\ b &\equiv -4\pi h_2 / \sqrt{.10 \rho_2 T} \end{aligned} \quad (3.12)$$

At $T = T_1$, $a = -\pi/2$. For $T < T_1$, $a < -\pi/2$; for $T > T_1$, $-\pi/2 < a < 0$. As $T \rightarrow \infty$, $a \rightarrow 0_-$.

Defining $\Delta R_j = R_{j+1} - R_j$, then from (3.11),

$$\Delta R_1 \Big|_{T=T_1} = \frac{\kappa_2 (1 - \kappa_1^2) e^{(b - \pi/2)} \sin(b)}{1 + 2\kappa_1 \kappa_2 e^b \cos(b) + (\kappa_1 \kappa_2 e^b)^2} \quad (3.13)$$

$$b = -\pi/2 \frac{h_2}{h_1} \sqrt{\rho_1/\rho_2} \quad (3.14)$$

Consider the case $\rho_2 \gg \rho_1$ (normally $h_2 \sim h_1$ and $\sin(b)$ is always negative.) and $\kappa_2 < 0$. $\Delta R_1 > 0$ and the effect of the correction for the third layer pulls the curve upward. However, for $\kappa_2 > 0$, R_1 is negative and less significant than for $\kappa_2 < 0$. For more complicated models, the process is equivalent to making $\Delta R_j \leq \delta$ for all values of T , where δ is determined by the scatter in the data.

In order to estimate h_2 from T_2 , one takes only the principal part of (3.10), which is equivalent to the process of Nabetani and Rankin (1969):

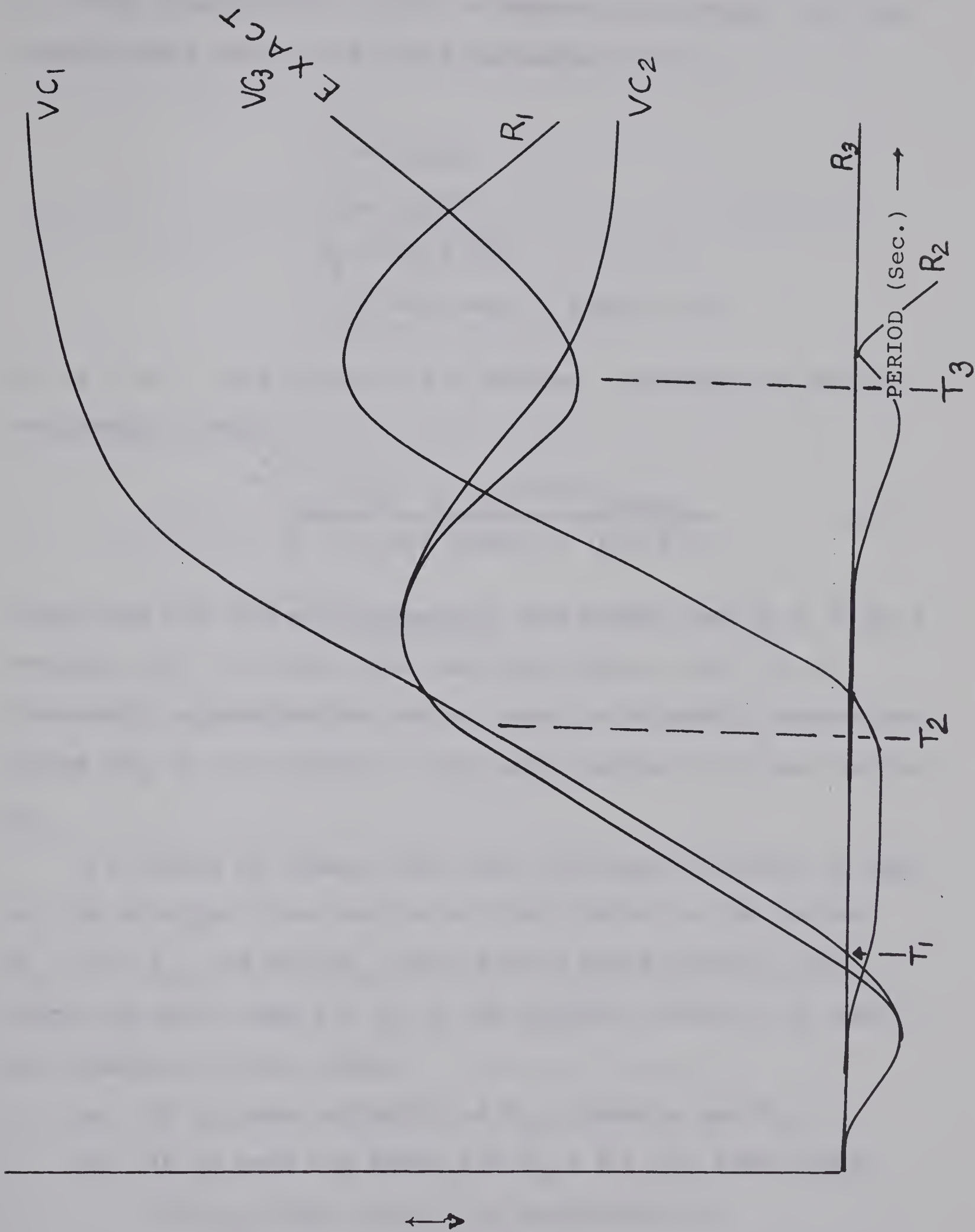
$$\begin{aligned} \text{REAL}(\text{EXP}[-Q(W_1 + W_2)]) \Big|_{T=T_2} &= 0 \\ Q(W_1 + W_2) \Big|_{T+T_2} &= \pi/2 \end{aligned} \quad (3.15)$$

For $T < T_2$, $(a + b) < -\pi/2$; for $T > T_2$, $-\pi/2 < (a+b) < 0$. As $T \rightarrow \infty$, $(a+b) \rightarrow 0_-$. It can be seen from expression (3.11) that if one chooses the point at which $R_1 = R_2$, then our layer thickness would be given by

$$\begin{aligned} \kappa_1 \kappa_2 e^b \cos(a) &= -\cos(a + b), \\ \text{or } h_2 &= \frac{\sqrt{10} \rho_2 T_2}{4\pi} \{ \cos^{-1}[-\kappa_1 \kappa_2 e^b \cos(a)] - a \} \end{aligned} \quad (3.16)$$

The relationships for the thicknesses of subsequent layers would be more involved. The numerical approximation involved

FIGURE 6: Choosing T_2 for model (3.5)



in using relationship (3.15) is demonstrated below. In the hypothetical model (3.5), the parameters are:

$$\kappa_1 = 0.818$$

$$\kappa_2 = -0.635$$

$$T_1 = 16.0 \text{ sec.}$$

$$T_2 = 41.0 \text{ sec. , from (3.15)}$$

If $(a + b) = -\pi/2$, then (3.11) becomes, according to Nabetani and Rankin (1969):

$$\Delta R_1 = \frac{\kappa_1 \kappa_2^2 (1 - \kappa_1^2) e^{(a+2b)} \cos(a)}{1 + 2\kappa_1 \kappa_2 e^b \cos(b) + (\kappa_1 \kappa_2 e^b)^2} \quad (3.17)$$

Inserting the correct parameters, one finds that at $T_2 = 41.0$ seconds, $\Delta R_1 = +0.004$, thus verifying that (3.15) is a reasonable approximation and as shown in FIGURE 6, causes the curve VC_2 to fit closely to the exact curves up to and beyond T_2 .

κ_1 should be chosen such that its slope is equal to that of the straight-line section of the V curve in the region $T_1 < T < T_2$; and the VC_2 curve should match exactly the V curve up until some $T > T_2$ if the correct values of T_1 and T_2 are chosen. If not, then

- a) if it does not match at T_1 , choose a new T_1 ;
- b) if it does not match for $T_1 < T < T_2$, then either
 - (i) T_2 (that is, h_2) is incorrect; or
 - (ii) κ_1 is incorrect.

When this section of the curve is matched, one goes on to the third approximation, if needed. When this is done, the curve adjustment is:

$$\begin{aligned} \Delta R_2 &= \frac{\kappa_1 e^{-QW_1} + \kappa_2 e^{-Q(W_1+W_2)} + \kappa_3 e^{-Q(W_1+W_2+W_3)} + \kappa_1 \kappa_2 \kappa_3 e^{-Q(W_1+W_3)}}{1 + \kappa_1 \kappa_2 e^{-QW_2} + \kappa_1 \kappa_3 e^{-Q(W_2+W_3)} + \kappa_2 \kappa_3 e^{-QW_3}} \\ &\quad - \frac{\kappa_1 e^{-QW_1} + \kappa_2 e^{-Q(W_1+W_2)}}{1 + \kappa_1 \kappa_2 e^{-QW_2}} \\ &= \frac{\kappa_3 e^{-Q(W_1+W_2+W_3)} (1 - \kappa_1^2) (1 - \kappa_2^2)}{\text{DENOMINATOR}} \end{aligned} \quad (3.18)$$

In a similar manner,

$$\Delta R_3 = \frac{\kappa_1 e^{-Q(W_1+W_2+W_3+W_4)} (1 - \kappa_1^2) (1 - \kappa_2^2) (1 - \kappa_3^2)}{\text{DENOMINATOR}} \quad (3.19)$$

Generally, the curve adjustment between successive approximations is:

$$\Delta R_{j-1} = [VC_j - VC_{j-1}] = \frac{\kappa_j (e^{-Q \sum_{i=1}^j W_i})^{\frac{j-1}{j}} \prod_{m=1}^{j-1} (1 - \kappa_m^2)}{\text{DENOMINATOR}} \quad (3.20)$$

and as has been previously stated, the process is continued until $R_j < \delta$, the scatter in the data.

In order to compute the successive thicknesses, one repeats the process leading to equations (3.8) and (3.15):

$$4\pi \left(\frac{h_1}{\sqrt{10} \rho_1 T_2} + \frac{h_2}{\sqrt{10} \rho_2 T_2} \right) = \pi/2 \quad (3.15)$$

Thus,

$$\begin{aligned}
 h_2 &= \sqrt{10 \rho_2 T_2}/8 - h_1 \sqrt{\rho_2/\rho_1} \\
 &= \sqrt{10 \rho_2 T_2}/8 - \sqrt{10 \rho_1 T_1}/8 \sqrt{\rho_2/\rho_1} \\
 &= \sqrt{10 \rho_2}/8 [\sqrt{T_2} - \sqrt{T_1}]
 \end{aligned} \tag{3.21}$$

and in general,

$$h_i = \sqrt{10 \rho_i}/8 [\sqrt{T_i} - \sqrt{T_{i-1}}] \tag{3.22}$$

This method of interpretation is implemented using interactive programming, which is described in the next chapter.

CHAPTER 4

RESULTS AND SUGGESTIONS FOR FURTHER WORK

The method of sequential layering was applied to several representative horizontally-stratified earth models; the main computer program listings are given in APPENDIX C.

FIGURE 7:

As can be seen, the third layer has a low resistivity compared with that of the second layer. Thus, T_1 is chosen to the right of the rightmost zero crossing. The curve follows parallel to the model in the straight-line region of 30-60 seconds period. T_2 is chosen while R_1 is less than zero. The second approximation corrects for the previous one and follows the curve until periods of over 1000 seconds. At T_3 , R_2 is greater than zero and the third approximation corrects for the rest of the curve.

FIGURE 8:

As before, R_1 is less than zero at T_1 and T_2 . It should be noted that because of poor contrasts, the curve has little "character" and therefore the data could be fitted satisfactorily by a range of values of h_2 and ρ_2 .

FIGURE 9:

The third layer has a relatively high resistivity and there is thus an inflexion in the curve. Since there is little resistivity contrast in the top two layers and the second layer is thick, T_1 can be chosen right at the zero crossing.

Since ρ_3 is greater than ρ_2 , R_1 is less than zero at T_2 .

FIGURES 10, 11, and 12:

In all curves with a relatively resistive upper layer, the first approximation followed the curve closely, unlike the previously-shown examples. The previous pattern was generally seen: if the model consisted of alternating layers of high and low resistivities, values of T were chosen before the residual reached zero; otherwise, after T was zero. T_2 in FIGURE 12 is an exception due to the fact that the effect of the third layer is small.

It was found that the most important requirement for grid matching was experience with the graphics display. The results shown previously were far superior to any obtained by other techniques in use at the time of writing. This method of inverse analysis is appealing for its heuristic merits; the assumptions of least-squares methods are unnecessary; the obviation of complex iterative techniques is its greatest actual saving. For instance, the operator may match a fairly complicated curve quite well using less than half of a minute of actual computing time.

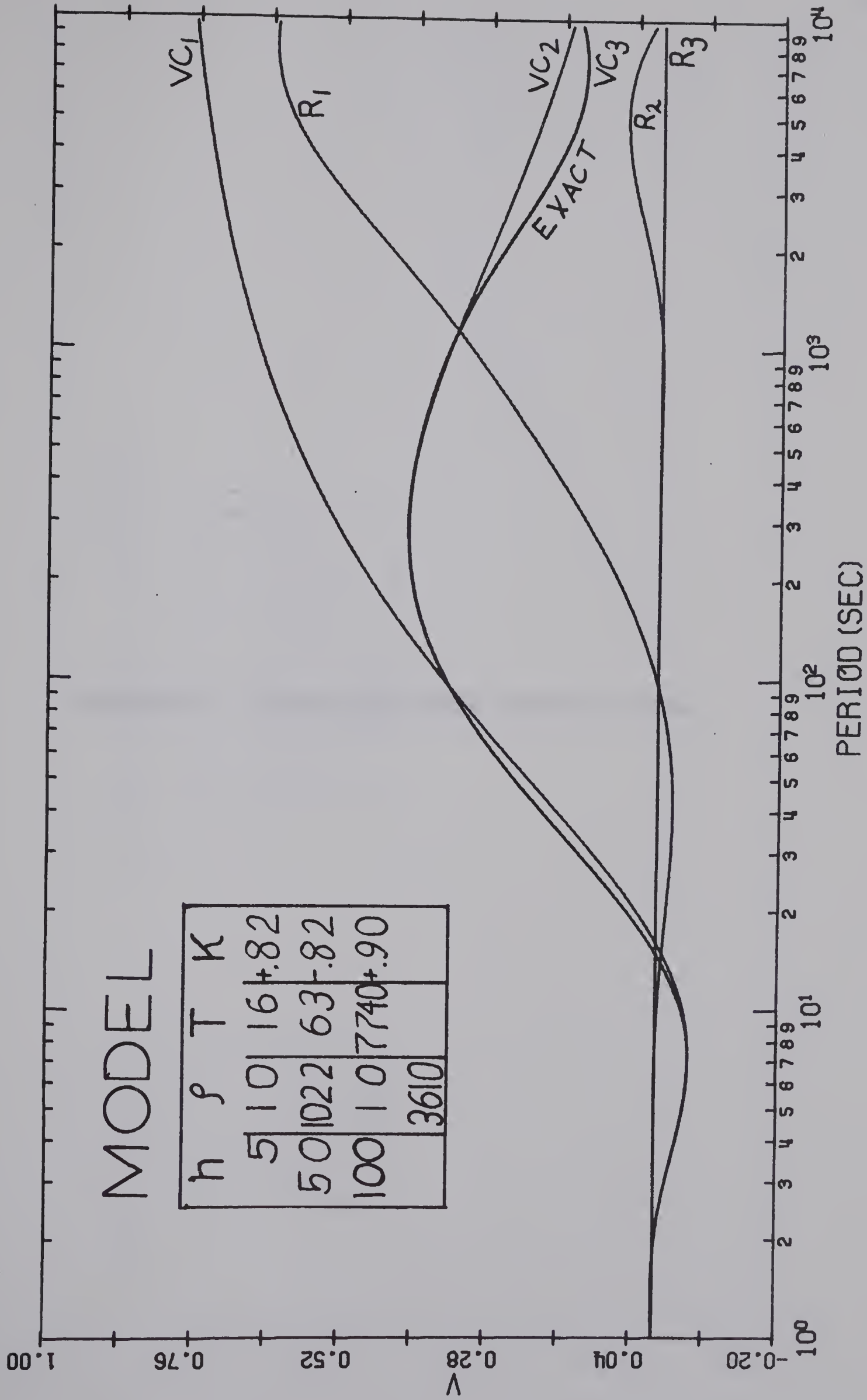
To date, the techniques for interpretation of the resistivity structure of the earth have been based on the calculation of apparent resistivity, which involves calculation of the amplitudes of the fields; thus, phase information was not required in the measurements. Since the technique presented

here is based on the calculation of the real part of the fields, both phase and amplitude information must be known. In future field work, care must be taken to obtain accurate values for the phase.

FIGURE 7: Four-layer demonstration model

MODEL

| h | ρ | T | K |
|-----|--------|------|-----------|
| 5 | 10 | 16 | $\pm .82$ |
| 50 | 1022 | 63 | $\pm .82$ |
| 100 | 10 | 7740 | $\pm .90$ |
| | 3610 | | |



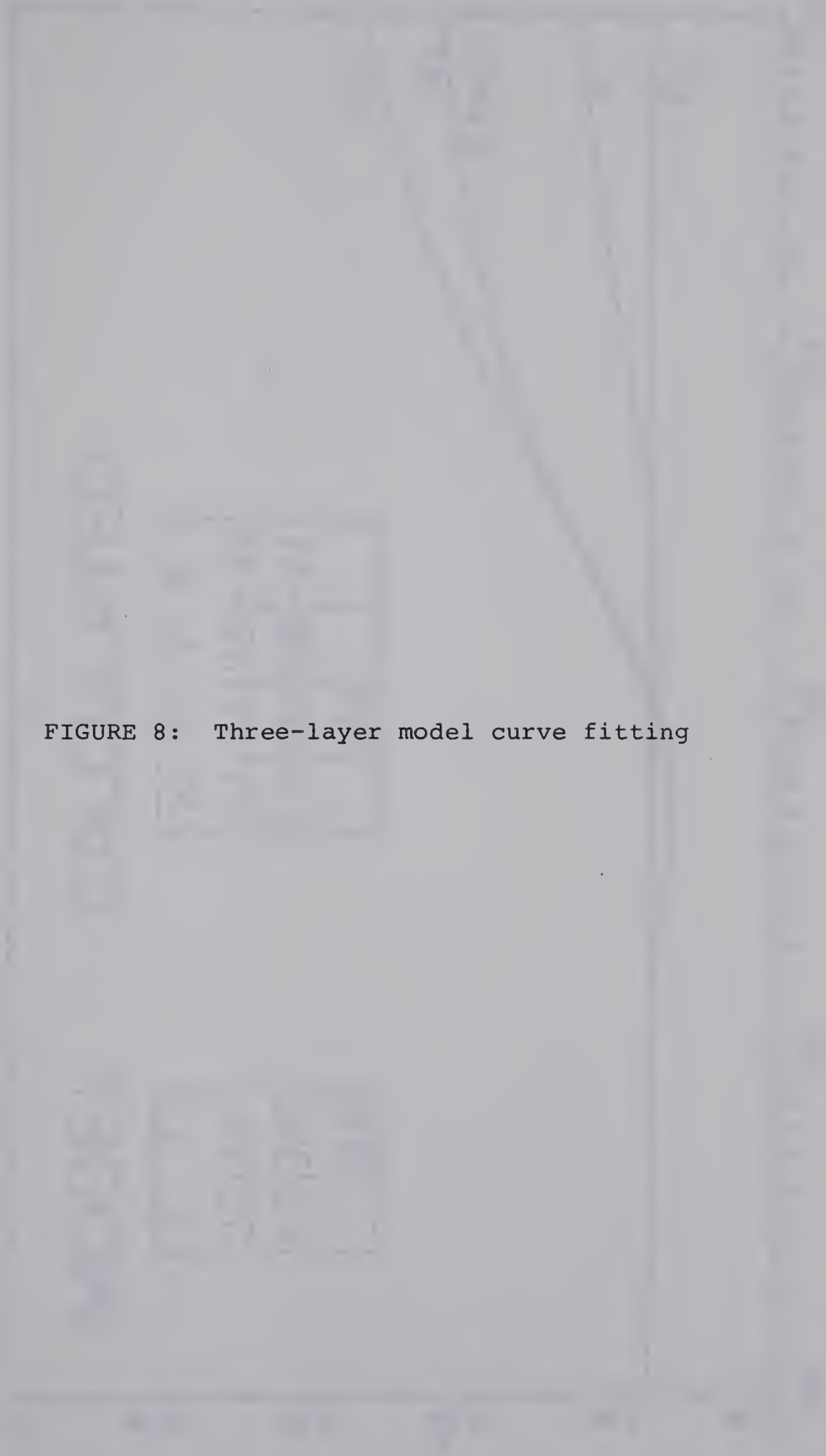


FIGURE 8: Three-layer model curve fitting

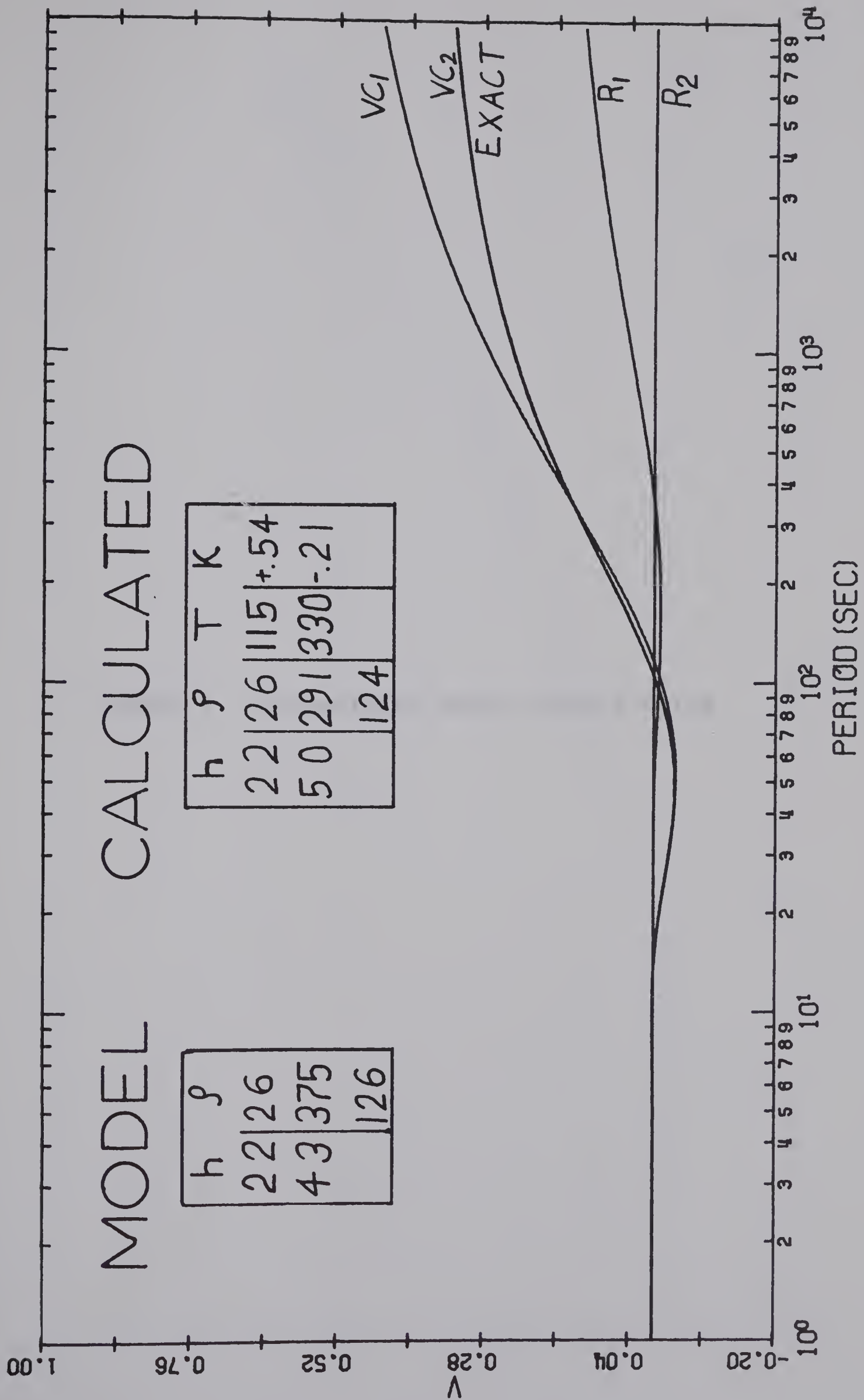


FIGURE 9: Three-layer model curve fitting

MODEL CALCULATED

| h | p |
|----|------|
| 5 | 10 |
| 50 | 50 |
| | 1000 |

| h | p | T | K |
|----|-----|-----|------|
| 5 | 10 | 16 | 4.38 |
| 49 | 50 | 470 | 4.63 |
| | 962 | | |

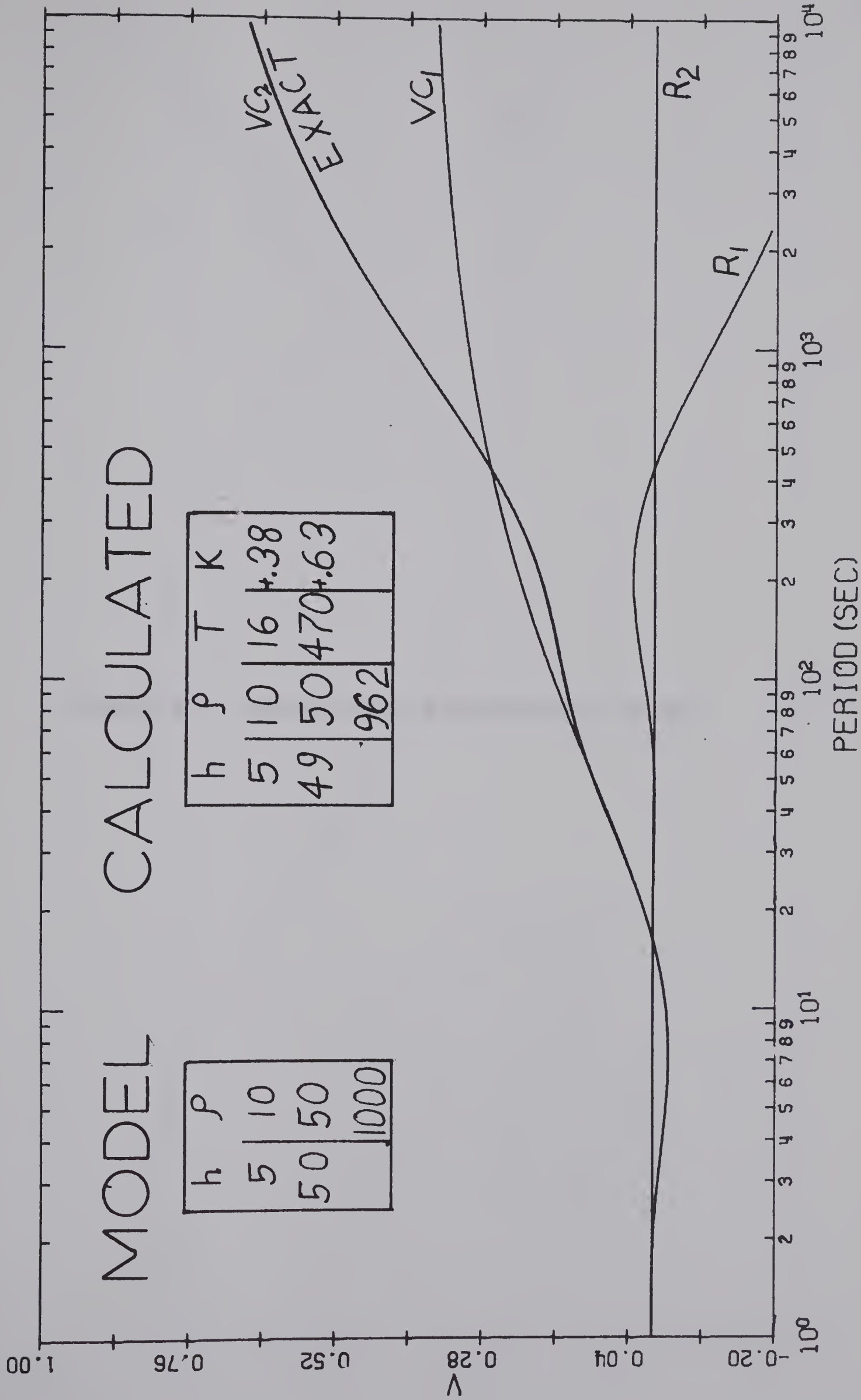


FIGURE 10: Three-layer demonstration model

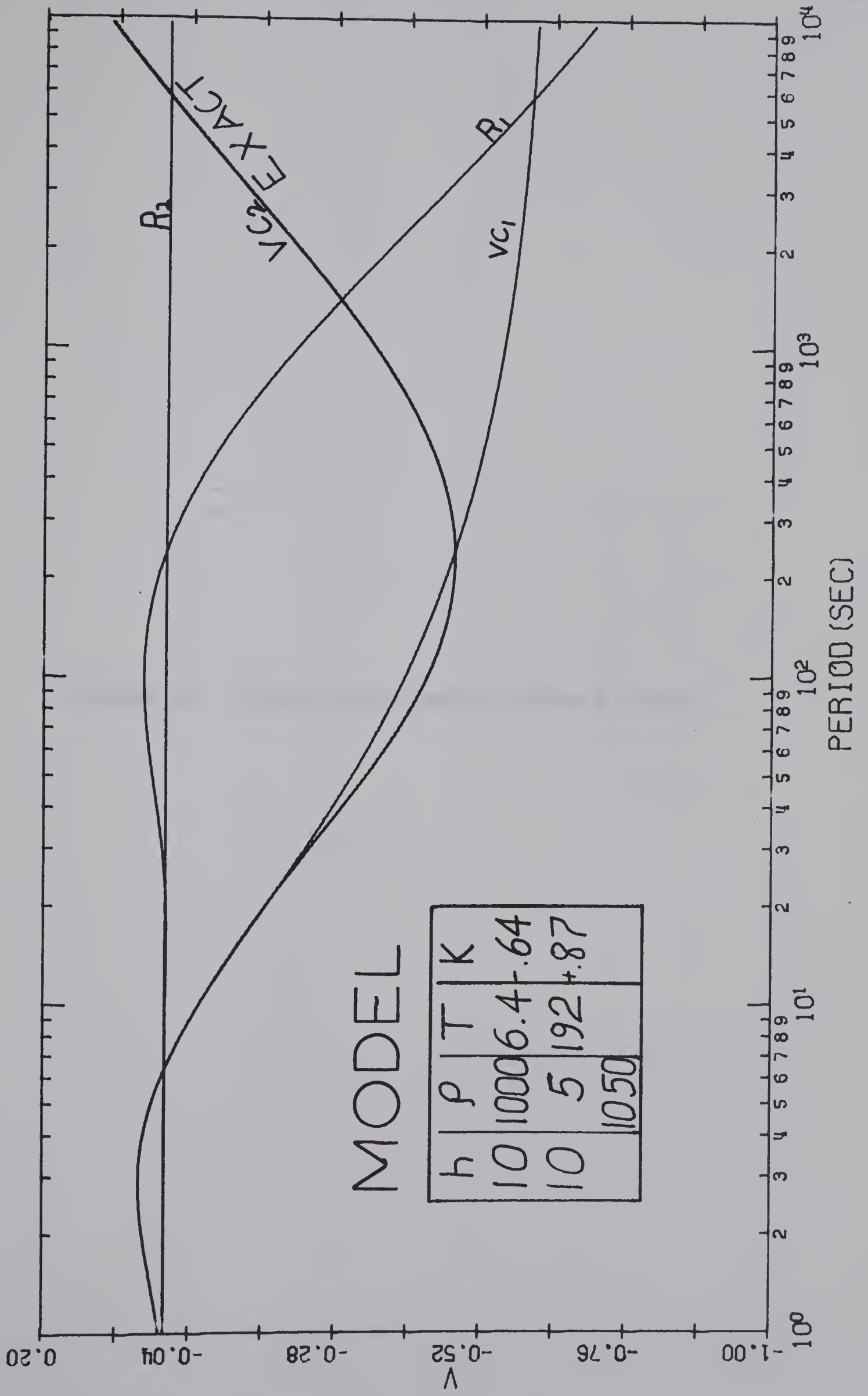
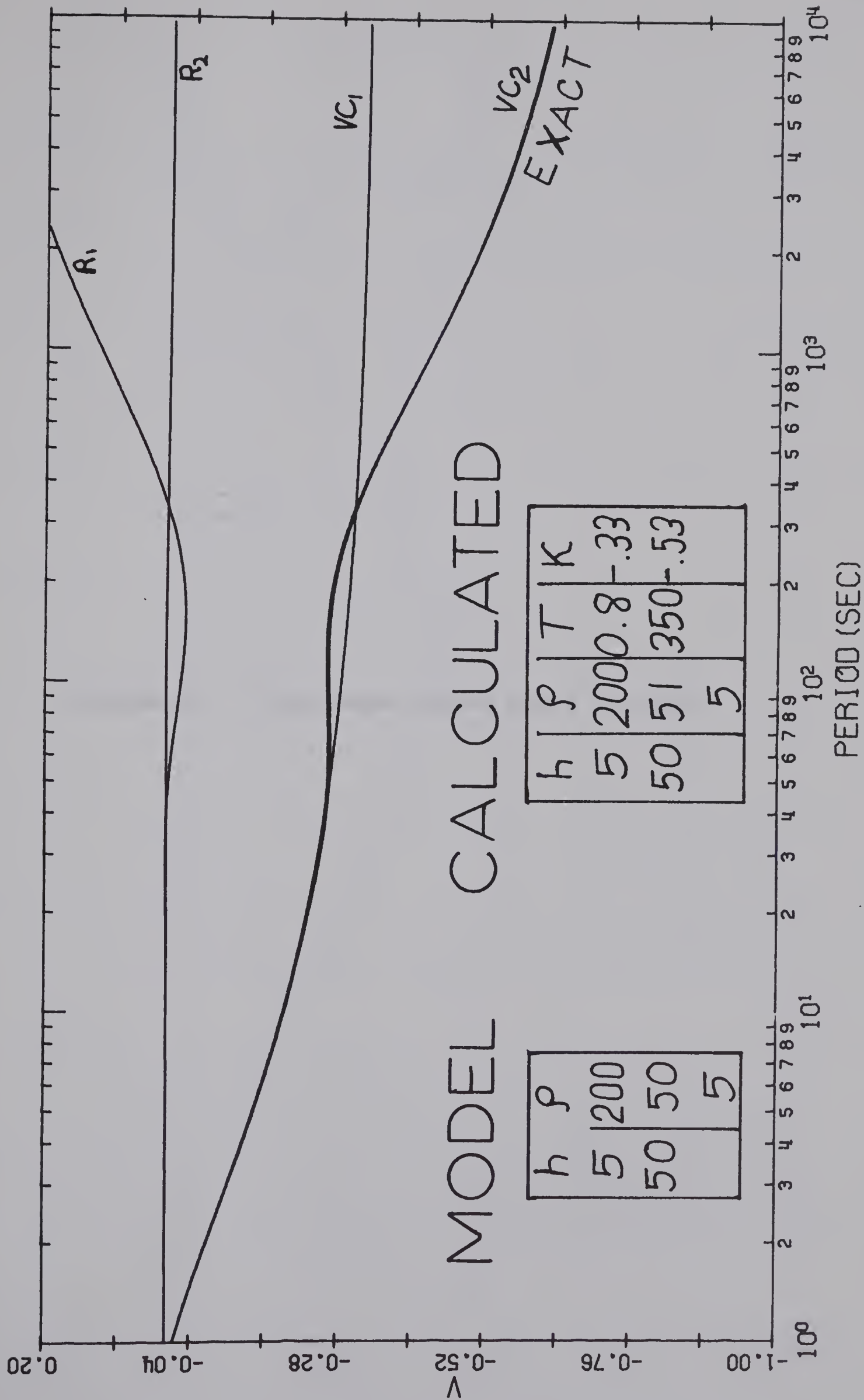


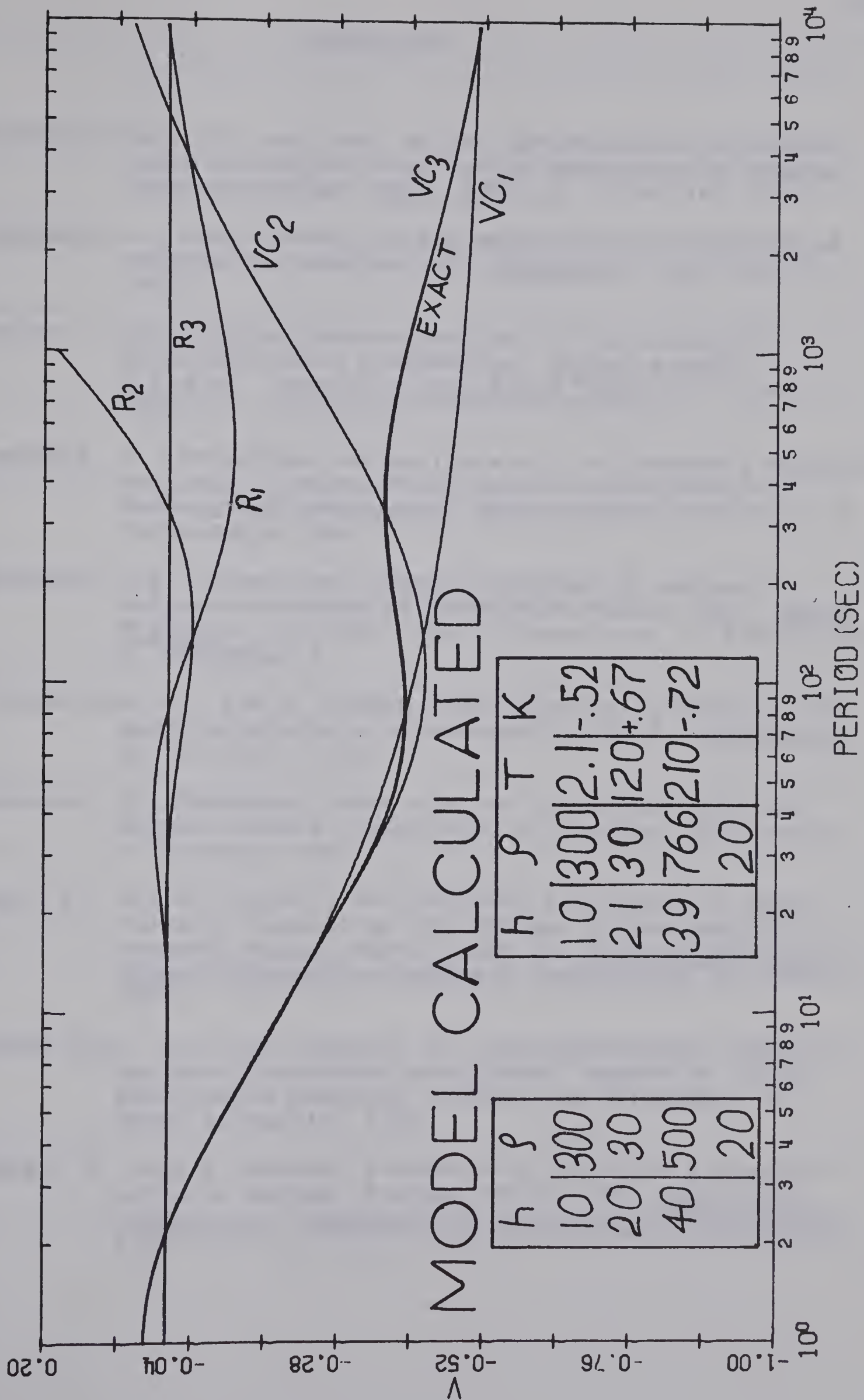
FIGURE 11: Three-layer model curve fitting



| h | p | T | K |
|----|-----|-----|-------|
| 5 | 200 | 0.8 | -0.33 |
| 50 | 51 | 350 | -0.53 |
| | 5 | | |

| h | p |
|----|-----|
| 5 | 200 |
| 50 | 50 |
| | 5 |

FIGURE 12: Four-layer model curve fitting



| h | ρ |
|-----|--------|
| 10 | 300 |
| 20 | 30 |
| 40 | 500 |
| | 20 |

| h | ρ | T | K |
|-----|--------|-----|-----|
| 10 | 300 | 2.1 | -52 |
| 21 | 30 | 120 | +67 |
| 39 | 766 | 210 | -72 |
| | 20 | | |

REFERENCES

- Bostick, F.X., Jr., and H.W. Smith, Investigation of large-scale inhomogeneities in the earth by the magnetotelluric method, Proc. IRE, 50, 2339-2346, 1962.
- Cagniard, L., Basic theory of the magnetotelluric method of geophysical prospecting, Geophysics, 18, 605-635, 1953.
- Chetaev, D.N., On the inverse problem in the theory of magnetotelluric prospecting, Akademia Nauk. S.S.S.R., Physics of the Solid Earth, 9, 610-611, 1966.
- Cantwell, T., Detection and analysis of low frequency magnetotelluric signals, Ph.D. thesis, Department of Geology and Geophysics, Massachusetts Institute of Technology, 1960.
- Dmitriev, V.N., Direct and inverse problems in magnetotelluric sounding of stratified media, Izv., Earth Physics, 1, 64-69, 1970. (Translated to English by F. Goodspeed.).
- d'Erceville, I., and G. Kunetz, The effect of a fault on the earth's natural electromagnetic field, Geophysics, 27, 651-665, 1962.
- Hasegawa, H., Magnetotelluric studies in central Alberta, Masters thesis, Department of Physics, University of Alberta, 1962.
- Kato, Y., and T. Kikuchi, On the phase difference of earth currents induced by the changes of the earth's magnetic field, Parts I and II, Science Reports of Tohoku University, Series 5, Geophysics, 2, 139-145, 1950.
- Laird, C.E., and F.X. Bostick, Jr., One-dimensional magnetotelluric inversion techniques: Report No. 101, Electronics Research Center, The University of Texas at Austin, 1970.
- Madden, T., and P. Nelson, A defence of Cagniard's magnetotelluric method, Project NR-371-401, Geophysics Laboratory, Massachusetts Institute of Technology, 1964.

- Marquardt, D.W., An algorithm for least-squares estimation of nonlinear parameters, J. Soc. Indust. Appl. Math. 11, 431-441, 1963.
- Nabetani, S., and D. Rankin, An inverse method of magnetotelluric analysis for a multilayered earth, Geophysics, 34, 75-86, 1969.
- Nelder, J.A., and R. Mead, A simplex method for function minimization, Computer Journal, 7, 308-313, 1964.
- Newman, M., Matrix computations, in Survey of Numerical Analysis, edited by Todd, J., New York, McGraw-Hill Book Co., Inc., p. 246.
- Patrick, F.W., Magnetotelluric Modeling Techniques, Ph.D. thesis, University of Texas at Austin, 1969.
- Patrick, F.W., and F.X. Bostick, Jr., Magnetotelluric modeling techniques; Report No. 59, Electronics Research Center, The University of Texas at Austin.
- Peeples, W.J., Magnetotelluric Profiling over a deep structure, Ph.D. dissertation, Department of Physics, The University of Alberta, 1969.
- Price, A.T., The theory of magnetotelluric methods when the source field is considered, J. Geophys. Res., 67, 1907-1918, 1962.
- Rankin, D., The magnetotelluric effect on a dike, Geophysics, 27, 666-676, 1962.
- Reddy, I.K., and D. Rankin, Magnetotelluric measurements in central Alberta, Geophysics, 36, 739-753, 1971.
- Rikitake, T., Electromagnetic induction within the earth and its relation to the electrical state of the earth's interior, Bull. Earthquake Res. Inst. Tokyo, 28, 45-98, 1950.
- Rikitake, T., Changes in earth currents and their relation to the electrical state of the earth's crust. Bull. Earthquake Res. Inst. Tokyo, 29, 270-275, 1951.
- Sims, W.E., Methods of magnetotelluric analysis, Ph.D. thesis, The University of Texas at Austin.
- Srivistava, S.P., Application of the magneto-telluric method to anisotropic and inhomogeneous bodies, J. Geophys. Res., 68, 5857-5868, 1963.

- Srivistava, S.P., Magnetotelluric two- and three-layer master curves, Publications of the Dominion Observatory, Ottawa, Volume 35, No. 7, 1967.
- Swift, C.M., A magnetotelluric investigation of an electrical conductivity anomaly in the southwestern United States, Ph.D. dissertation, Massachusetts Institute of Technology, 1967.
- Tikhonov, A.N., Determination of the electrical characteristics of deep layers of the earth's crust, Dok. Akad. Nauk., USSR, 73, 295-297, 1950.
- Tikhonov, A.N., Mathematical foundations of electromagnetic-sounding theory, USSR Computational Mathematics and Mathematical Physics, 5, No. 3, 207-211, 1965.
- Vozoff, K., H. Hasegawa, and R.M. Ellis, Results and limitations of magnetotelluric surveys in simple geologic situations, Geophysics, 28, 778-792, 1963.
- Wait, J.R., On the relation between telluric currents and the earth's magnetic field, Geophysics, 19, 281-289, 1954.
- Word, D.R., An investigation of the magnetotelluric tensor impedance method, Ph.D. thesis, The University of Texas at Austin, 1970.
- Word, D.R., Smith, H.W., and F.X. Bostick, Jr., An investigation of the magnetotelluric tensor impedance method: Report No. 82, Electronics Research Center, The University of Texas at Austin, 1970.
- Wu, F.T., The inverse problem of magnetotelluric sounding, Geophysics, 33, 972-979, 1968.
- Yungul, S.H., Magnetotelluric sounding three-layer interpretation curves, Geophysics, 26, 465- 478, 1961.

APPENDICES

APPENDIX A

Solution of the Wave Equation for a Source of Finite Dimensions.

If the inducing magnetic field has an arbitrary distribution, the solution of (2.17) can be found, following Price (1962):

$$\vec{E} = e^{i\omega t} \zeta(z) \vec{F}(x, y) \quad (A.1)$$

where

$$\vec{F}(x, y) = (\partial P / \partial y, -\partial P / \partial x, 0) \quad (A.2)$$

so that equation (2.9) is satisfied and $\vec{E}_z = 0$, because the layers of equal conductivity are parallel to the surface and thus the induced currents flow parallel to the surface of the earth (that is, in the x-y plane).

Substituting (A.1) into equation (2.17),

$$\begin{aligned} \nabla^2 \vec{E} &= e^{i\omega t} \left\{ \zeta(z) \left[\frac{\partial^2 \vec{F}(x, y)}{\partial x^2} + \frac{\partial^2 \vec{F}(x, y)}{\partial y^2} \right] + \vec{F}(x, y) \frac{d^2 \zeta(z)}{dz^2} \right\} \\ &= k^2 e^{i\omega t} \zeta(z) \vec{F}(x, y) \end{aligned} \quad (A.3)$$

or

$$\frac{1}{F(x, y)} \frac{\partial^2 F(x, y)}{\partial x^2} + \frac{\partial^2 F(x, y)}{\partial y^2} = k^2 - \frac{1}{\zeta(z)} \frac{d^2 \zeta(z)}{dz^2} \quad (A.4)$$

Since both sides of equation (A.4) are independent, they can be equated to the constant $-\nu^2$. The resultant equations are

$$\frac{\partial^2 F(x,y)}{\partial x^2} + \frac{\partial^2 F(x,y)}{\partial y^2} + v^2 F(x,y) = 0 \quad (\text{A.5})$$

and

$$\frac{d^2 \zeta(z)}{dz^2} = (v^2 + k^2) \zeta(z) \quad (\text{A.6})$$

where v is known as the "source dimension factor", which goes to zero for plane waves.

Matrix Computation for Calculation of Surface Impedance

The matrix M in equation (2.51) can be rewritten according to Newman (1962)

$$\begin{array}{ccccccc}
 b_1 & c_1 & & & & & \\
 a_1 & b_2 & c_2 & & & & \\
 & a_2 & b_3 & c_3 & & & \\
 & & \cdot & & & & \\
 & & \cdot & \cdot & & & \\
 & & \cdot & \cdot & \cdot & & \\
 & & & \cdot & & & \\
 & & & a_{2n-1} & b_{2n} & c_{2n} & \\
 & & & & a_{2n} & b_{2n+1} & c_{2n+1} \\
 & & & & & a_{2n+1} & b_{2n+2}
 \end{array}
 \tag{B.1}$$

where

$$\begin{aligned} a_1 &= 1 + \kappa_0 & a_2 &= \exp[-k_1 z_1] & a_3 &= (1 + \kappa_1) \exp[k_1 z_1] \\ a_4 &= \exp[-k_2 z_2] \dots a_{2n} &= \exp[-k_n z_n] & a_{2n+1} &= (1 + \kappa_n) \exp[k_n z_n] \\ b_1 &= -\kappa_0 & b_2 &= -\kappa_0 & b_3 &= -\kappa_1 \exp[k_1 z_1] \\ b_4 &= -\kappa_1 \exp[-k_2 z_1] \dots b_{2n+1} &= -\kappa_n \exp[k_n z_n] & b_{2n+2} &= -\kappa_n \exp[-k_{n+1} z_n] \\ c_1 &= 1 & c_2 &= -1 & c_3 &= (\kappa_1 - 1) \exp[-k_2 z_1] \\ c_4 &= -\exp[k_2 z_1] \dots c_{2n} &= -\exp[k_{n+1} z_n] & c_{2n+1} &= (\kappa_n - 1) \exp[-k_{n+1} z_n] \end{aligned}$$

(B.2)

Minors of this matrix are:

$$\begin{aligned}
 D_0 &= 1 \\
 D_1 &= b_1 \\
 &\vdots \\
 D_k &= b_k D_{k-1} - a_{k-1} c_{k-1} D_{k-2}, \quad 2 \leq k \leq 2n+2.
 \end{aligned}
 \tag{B.3}$$

Thus,

$$D_{2n+2} = -\kappa_n \exp[-k_{n+1} z_n] D_{2n+1} + (1 - \kappa_n) \exp[-(k_{n+1} - k_n) z_n] D_{2n}
 \tag{B.4}$$

and

$$D_{2n+1} = -\kappa_n \exp[k_n z_n] D_{2n} + \exp[-k_n (z_n - z_{n-1})] D_{2n-1}
 \tag{B.5}$$

for even and odd minors respectively. Substituting (B.5) into (B.4) gives

$$D_{2n+2} = \exp[-(k_{n+1} - k_n) z_n] D_{2n} - \kappa_n \exp[-(k_{n+1} + k_n) z_n + k_n z_{n-1}] D_{2n-1}.
 \tag{B.6}$$

The determinant $\det M_{11}$ of the submatrix M_{11} , formed by omitting the first row and column of M , can be treated similarly to obtain

$$D'_{2n} = -\kappa_n \exp[k_n z_n] D'_{2n-1} + \exp[-k_n (z_n - z_{n-1})] D'_{2n-2}
 \tag{B.7}$$

$$D'_{2n+1} = \exp[-(k_{n+1} - k_n) z_n] D'_{2n} - \kappa_n \exp[-(k_{n+1} + k_n) z_n + k_n z_{n-1}] D'_{2n-2}
 \tag{B.8}$$

$$\begin{aligned}
D_0 &= 1 \\
D_1 &= -\kappa_0 \\
D_2 &= 1 \\
D_3 &= -\kappa_0 \exp[-k_1 z_1] - \kappa_1 \exp[k_1 z_1] \\
D_4 &= \exp[-(k_2 - k_1) z_1] + \kappa_0 \kappa_1 \exp[-(k_2 + k_1) z_1] \\
&\vdots
\end{aligned} \tag{B.9}$$

$$\begin{aligned}
D'_0 &= 1 \\
D'_1 &= -\kappa_0 \\
D'_2 &= \exp[-k_1 z_1] + \kappa_0 \kappa_1 \exp[k_1 z_1] \\
D'_3 &= -\kappa_0 \exp[-(k_2 - k_1) z_1] - \kappa_1 \exp[-(k_2 + k_1) z_1] \\
&\vdots
\end{aligned} \tag{B.10}$$

Then equation (2.56) of the text can be written as

$$\left. \frac{E_x}{i\omega H_y} \right|_{z=0} = \frac{1}{k_0} \frac{D_{2n+2} - D'_{2n+1}}{D_{2n+2} + D'_{2n+1}} \tag{B.11}$$

APPENDIX C

2 CONTINUE

C

WRITE(6,201) NLayer

201 FORMAT(40X,I2,' LAYERED ISOTROPIC EARTH'/)

C

WRITE(6,202)(F(I),S(I),I = 1,NLayer)

202 FORMAT(40X,F10.2,5X,F10.2)

C

WRITE(6,205)

205 FORMAT(//)

C

WRITE(6,204)

204 FORMAT(2(2X,'T(SEC)',4X,'SQRT(T)',4X,'GAMMA',12X,'V',5X))

C

WRITE(6,205)

C

WRITE(6,203)(T(M),IT(M),RGAM(M),V(M),M=1,NPERD)

203 FORMAT(2(F10.3,5X,F10.3,5X,F10.3,5X,F10.3))

C

IDU = 8

NUPLDT = 1

CALL GPL(T,V,V,NPERD,NUPLDT,2,1,5,3,0.,4.,9.,

C=.2,.24,5.,DELTA,IDU)

10 CONTINUE

C

C

C

C

C

C

FPI = 12.5565706

SIG = 1./SQRT(K(1))

H1 = SQRT(R(1)*T1*10.)/8.

HH = FPI*H1*SIG

C

C

WRITE(6,1371)H1

1371 FORMAT(10X,'H1 =',F8.3//)

C

C

C WE NOW BEGIN CALCULATION OF THE TWO-LAYER APPROXIMATION,

C WHICH DEPENDS ON THE OBSERVED VALUE OF T1, THE "RIGHT-

C MOST ZERO-CROSSING OF THE TIME AXIS BY THE FUNCTION V.

C NOW THAT WE HAVE THE VALUES FOR THE MODEL, WE SHALL

C CALCULATE THE VALUES OF THE FIRST APPROXIMATION,

C WHICH IS ESSENTIALLY A 2-LAYER CURVE. THIS CURVE

C SHOULD FIT THE MODEL CURVE UP TO A PERIOD T2.

C THE CALCULATIONS ARE STRAIGHTFORWARD AND EXACTLY AS

C LAID OUT IN THE MCFESEN THESIS.

C

C

C

DO 1300 J = 1,NPERD

ARG(J) = -HH/SQRT(10.*T(J))

FN(J) = EXP(ARG(J))*CES(ARG(J))


```
WRITE(6,1354)T3
```

C

C

$$FRAC_2 = (1. - KAY_3) / (1. + KAY_3)$$


```

R(4) = R(3)/(FRAC2)**2.
F4 = SQRT(R(+)/R(L))*(SQRT(10.*R(1)*T4)/B. - FRAC*H2/
C-FRAC*FRAC1*H3 - H1)

```

C

C

```

DO 1610 J = 1,NPERD
ARC3(J) = ARG2(J)*FRAC2*H4/H3
FN3(J) = EXP(ARG3(J))*COS(ARG3(J))
FN3C(J) = EXP(ARG3(J))*C*SIN(ARG3(J))
VTTTT(J) = KAY4*FN3(J)
V4(J) = V1C(J) + VTTTT(J)*FN(J)*FN1(J)*FN2(J)
V4CC(J) = (V1CC(J) + KAY2/KAY1*V1CC(J)*(FN1(J) + FN1C(J)) +
CKAY3/KAY1*V1CC(J)*(FN1(J) + FN1C(J))*(FN2(J) + FN2C(J)) +
CKAY4/KAY1*V1CC(J)*(FN1(J) + FN1C(J))*(FN2(J) + FN2C(J))*(FN3(J) +
CFN3C(J)) + KAY2*KAY3*V1CC(J)*(FN2(J) + FN2C(J)) + V1CC(J)*
C(FN2(J) + FN2C(J))*(FN3(J) + FN3C(J))*KAY2*KAY4 + V1CC(J)*KAY3*
CKAY4*(FN3(J) + FN3C(J)) + KAY2*KAY3*KAY4/KAY1*V1CC(J)*(FN1C(J)
C+FN1(J))*(FN3(J) + FN3C(J)))/(1. + KAY2*KAY1*(FN1(J) + FN1C(J))
C+KAY1*KAY3*(FN1(J) + FN1C(J))*(FN2(J) + FN2C(J)) + KAY2*KAY1*
C(FN2(J) + FN2C(J)) + KAY1*KAY4*(FN1(J) + FN1C(J))*(FN2(J) +
CFN2C(J))*(FN3(J) + FN3C(J)) + KAY2*KAY4*(FN2(J) + FN2C(J))*
C(FN3(J) + FN3C(J)) + KAY3*KAY4*(FN3(J) + FN3C(J)) + KAY1*KAY2*
CKAY3*KAY4*(FN1(J) + FN1C(J))*(FN3(J) + FN3C(J)))
V4C(J) = REAL(V4CC(J))
F4(J) = V4(J) - V(J)
R4C(J) = V4C(J) - V(J)
1610 CONTINUE

```

C

C

```

WRITE(6,1363)T4

```

```

1363 FORMAT(10X,'T4 =',F4.2//)

```

C

```

WRITE(6,1620)R(4)

```

```

1620 FORMAT(1X,'R(4) = ',F6.1//)

```

C

```

WRITE(6,1630)F4

```

```

1630 FORMAT(1X,'H4 = ',F5.2//)

```

C

C

```

R(5) = R(4)*(1. + KAY4)**2./(1.-KAY4)**2.

```

```

WRITE(6,1791)R(5)

```

```

1791 FORMAT(20X,'R(5) = ',F10.2//)

```

C

```

RES = 0.

```

```

DO 3880 J = 1,NPERD

```

```

RES = RES + (R4C(J))**2

```

```

3880 CONTINUE

```

```

SD = SQRT(RES/(NPERD-1.))

```

```

WRITE(6,3889)SD

```

```

3889 FORMAT(20X,'STANDARD DEVIATION = ',F10.2//)

```

C

C

```

WRITE(6,1640)KAY4

```

```

1640 FORMAT(1X,'VALUES FOR THE FOURTH APPROXIMATION, WITH KAY4 = ',F5.2/
C/)

```


C

WRITE(6,205)

WRITE(6,1367)

```
1367 FORMAT(2EX,'T(SEC)',5X,'SQRT(T)',10X,'V4',15X,'R4',12X,'V4C',12X,  
C'R4C')
```

WRITE(6,205)

WRITE(6,150B)(T(M),TT(M),V4(M),R4(M),V4C(M),R4C(M),M=1,NPERM)

C

C

NUPLOT = 5

```
CALL GPL(T,V4C,V4C,NPERC,NUPLOT,2,1,5,3,3.,4.,3.,  
C-.2,.24,5.,DELTA,ICU)
```

NUPLOT = -9

```
CALL GPL(T,R4C,R4C,NPERC,NUPLOT,2,1,5,3,3.,4.,3.,  
C-.2,.24,5.,DELTA,ICU)
```

STOP

END

MEMORY REQUIREMENTS 010FEB BYTES


```
C
C
C      NLayer IS THE NUMBER OF LAYERS IN THE EARTH MODEL
C
16 WRITE(6,83)
83 FORMAT(' ENTER NLayer')
   READ(5,90) NLayer
C
C
C      IPDSN INDICATES HOW SCREEN COORDINATES MUST BE ESTABLISHED
C
   WRITE(6,111)
111 FORMAT(' ENTER 1 IF RESISTIVE CURVE; -1 IF CONDUCTIVE CURVE')
   READ(5,90) IPDSN
   IF(IPDSN .EQ. 1) IHERE = 100
   IF(IPDSN .EQ. -1) IHERE = 924
C
C
C      ESTABLISH RANGE ON X-AXIS
C
   WRITE(6,112)
112 FORMAT(' ENTER LOWEST VALUE ON X-AXIS')
   READ(5,92) XSCALE
   DO 50 I = 1, NPERD
   50 T(I) = T(I) * XSCALE
C
C
C      IN THIS SECTION WE CALCULATE OR READ IN VALUES OF "V" . . .
C
C      THE CALCULATION OF THE "V"-CURVE IS BASED ON THE CONTINUITY OF
C      THE ELECTRIC AND MAGNETIC FIELD COMPONENTS AT THE BOUNDARIES
C      BETWEEN THE HORIZONTAL LAYERS OF THE EARTH.
C      C      IS THE SQUARE ROOT OF -1.
C      TPI      IS 2*PI
C      A(NLayer) = 0. AND B(NLayer) = 1., CONSISTENT WITH THE FACT
C      THAT IN THE HALF-SPACE, THERE CAN BE NO REFLECTED WAVE AND
C      THE TRAVELING WAVE MUST DECAY. THE BULK OF THESE
C      CALCULATIONS COULD BE USED FOR CALCULATING THE APPARENT
C      RESISTIVITY AND PHASE ANGLE OF THE ELECTRIC FIELD WITH
C      RESPECT TO THE MAGNETIC FIELD. AFTER STATEMENT 5, WE HAVE
C      INSERTED THE CALCULATION FOR "V", THE MODEL CURVE.
C
C      IDAT = 0
C
C      INDICATE IF DATA CURVE TO BE SIMULATED OR REAL DATA
C
   WRITE(6,113)
113 FORMAT(' IF V IS TO BE SIMULATED, ENTER 1')
   READ(5,90) IDAT
   IF (IDAT .NE. 1) GO TO 250
C
C
C      H AND R FOR EACH LAYER IS ENTERED
```



```

C
      DO 100 I = 1, NLAYER
        WRITE(6,84) I
      84 FORMAT(' ENTER H AND E FOR LAYER ', I1)
      100 READ(5,91) H(I), E(I)
      91 FORMAT(2F10.1)
C
C
      250 C = (0.0, 1.0)
        TPI = 6.2831853
        FPI = 2.0*TPI
C
      DO 2 IJ = 1, NPERD
        CCMFGA = C*TPI/T(IJ)
        CK = -0.2*TPI*CCMFGA
        IF (IDAT .EQ. 0) GO TO 2
        A(NLAYER) = (0.0, 0.0)
        B(NLAYER) = (1.0, 0.0)
C
        NL1 = NLAYER - 1
        DO 3 J=1, NL1
          I = NL1 - J + 1
          H1 = H(I)
          K1 = CSQRT(CK/R(I))
          K2 = CSQRT(CK/R(I+1))
          P1 = (K1 + K2)/(2.*K1)
          P2 = (K1 - K2)/(2.*K1)
          P3 = -K1*H1
          P4 = K1*H1
C
          A(I) = P1*A(I+1)*CEXP(P3) + P2*B(I+1)*CEXP(P3)
          B(I) = P2*A(I+1)*CEXP(P4) + P1*B(I+1)*CEXP(P4)
        3 CONTINUE
C
        V(IJ) = REAL(A(1)/E(1))
      2 CONTINUE
C
      IF(IDAT .EQ. 1) GO TO 200
C
      V IS READ (REAL DATA)
C
      WRITE (6,114)
      114 FORMAT(' ENTER R(1)')
      READ(5,91) R(1)
C
      INSERT FACILITY TO READ DATA HERE
      85 FORMAT(10F10.3)
      200 SIG=1.0/SQRT(R(1))
        WRITE(6,101)
      101 FORMAT(21H DATA CURVE DISPLAYED)
C
C
      DISPLAY DATA CURVE
C
      CALL DELBLK(49)
      CALL BLOCK(49)
      CALL TEXT(F,1,1000,10,10'DATA CURVE,TR,F)

```



```
      CALL ENDBLK
      DO 300 I = 1, NPERD
      SCRENT = T(I)/XSCALE
      AX(I) = ALOG10(SCRENT) * 200
300  AY(I) = V(I) * 1000
      CALL ERSBK(1)
      CALL DELBLK(10)
      CALL BLOCK(10)
C
C   DATA CURVE
C
      CALL DLINE(F,F,AX,AY,NPERD,F,F)
C
C   X-AXIS
C
      CALL MOVE(F,0,0)
      CALL VECTOR(F,800,0,F,F)
      CALL ENDBLK
      CALL DISPLY(10,1,0,IHERE)
      CALL DISPLY(49,1,0,0)
310  CALL TRANMT
      CALL ERSBK(52)
C
C   A VALUE OF K MUST BE ENTERED AT GRID KEYBOARD . . .
C
      CALL CALPHA(1,IX,IY,NUM,10,STRING,&32))
C
C   . . . OTHERWISE ERROR MESSAGE APPEARS
C
309  CALL RSTBK(52)
      GO TO 310
C
320  CALL KP (KAY1,K(1),F(2),STRING,NUM,1,2,&309)
C
C   T1 IS ENTERED AT TERMINAL KEYBOARD
C
      17 WRITE(6,31)
      81 FORMAT(' ENTER T1')
      READ(5,93) T1
      93 FORMAT(F10.2)
C
C
C   H1 CALCULATED AND PRINTED
C
      H1 = SQRT(F(1)*T1*10.0)/B.
      WRITE(6,103) H1
103  FORMAT(6H H1 = ,F10.2)
      HH = FPI*H1*SIG
C
C   FLASHING * AT T ON THE X-AXIS
C
      IT1 = 200*ALOG10(T1)/XSCALE
      CALL DELBLK(3)
      CALL BLOCK(3)
      CALL TEXT(F,IT1,0,1,1H*,TR,TR)
```



```
CALL ENDBLK
CALL DISPLY(3,1,0,IFEX5)
```

```
C
C
```

```
C *****
C *****
C *****
```

```
C WE NOW BEGIN CALCULATION OF THE TWO-LAYER APPROXIMATION
C WHICH DEPENDS ON THE OBSERVED VALUE OF T1, THE "RIGHT-
C MOST ZERO-CROSSING OF THE TIME AXIS BY THE FUNCTION V.
C NOW THAT WE HAVE THE VALUES FOR THE MODEL, WE SHALL
C CALCULATE THE VALUES OF THE FIRST APPROXIMATION,
C WHICH IS ESSENTIALLY A 2-LAYER CURVE. THIS CURVE
C SHOULD FIT THE MODEL CURVE UP TO A PERIOD T2.
C THE CALCULATIONS ARE STRAIGHTFORWARD AND EXACTLY AS
C LAID OUT IN THE MOZESON THESIS.
```

```
C
C
C
C
```

```
1000 DO 1300 J=1,NPERM
      ARG(J) = -HF/SQRT(10.*T(J))
      FN(J) = EXP(ARG(J))*COS(ARG(J))
      FNC(J) = EXP(ARG(J))*C*SIN(ARG(J))
      VICC(J) = KAY1*(FNC(J) + FN(J))
      VT(J) = KAY1*FN(J)
      V1(J) = VT(J)
      VIC(J) = VICC(J)
      R1(J) = V1(J) - V(J)
      RIC(J) = VIC(J) - V(J)
1300 CONTINUE
      FRAC = (1.-KAY1)/(1.+KAY1)
```

```
C
C
```

```
DISPLAY FIRST APPROXIMATION
```

```
C
```

```
1800 CALL DELBLK(49)
      CALL BLCK(49)
      CALL TEXT(F,1,1000,19,19HFIRST APPROXIMATION,TR,F)
      CALL ENDBLK
      CALL GRID(1,T2,KAY1,KAY2,VIC,T,F(1),F(2),R(3),DN,NPERM,1,HERE,
      2XSCALE,&15,&1000,&1900,&2000)
```

```
C
```

```
C T AND H CALCULATED AND DISPLAYED
```

```
C
```

```
1900 H2 = 1./FRAC*(SQRT(10.*P(1)*T2)/8. -H1)
      WRITE(6,104) T2,H2
      CALL TH(T2,H2,IFEX,XSCALE)
      GO TO 1800
```

```
104 FORMAT(5H T2 = ,F10.2,10X,5H H2 = ,F10.2)
```

```
C
C
C
```

```
C >>>>><<<<<>>>><<<<<>>>><<<<<>>>><<<<<>>>><<<<<>>>>
C NEXT, WE CALCULATE THE THREE-LAYER APPROXIMATION, WHICH
C IS DEPENDENT UPON THE POINT AT WHICH THE FIRST APPROX-
```


2

C

1330

C

C

C

C

C

6

C

C

3.000


```
(KAY3*KAY4*(FN1(J) + FN1C(J))*(FN3(J) + FN3C(J)))  
V4C(J) = REAL(V4CC(J))  
R4(J) = V4(J) - V(J)  
R4C(J) = V4C(J) - V(J)
```

```
1600 CONTINUE
```

```
C
```

```
C
```

```
C
```

```
DISPLAY FOURTH APPROXIMATION
```

```
CALL DELBLK(49)
```

```
CALL BLOCK(49)
```

```
CALL TEXT(F,1,1000,20,20)FOURTH APPROXIMATION,TR,F)
```

```
CALL ENDBLK
```

```
CALL GRID(4,T4,KAY4,KAY5,V4C,T,F(4),F(5),F(6),DN,APEND,HERE,  
2XSCALE,&2000,&3000,&999,&999)
```

```
C
```

```
JOB TERMINATES NORMALLY IF ANY ATTEMPT TO CONTINUE
```

```
999 RETURN
```

```
END
```

MEMORY REQUIREMENTS 008274 BYTES

SUBROUTINE SCREEN

SUBROUTINE SCREEN INITIALIZES THE GRID DISPLAY

LOGICAL*1 TR/.TRUE./,F/.FALSE./

BLOCK 1 DISPLAYS THE APPROXIMATION CURVE

CALL BLOCK(1)

CALL TEXT(F,1,1,1,1HA,F,F)

CALL ENDBLK

BLOCK 2 DISPLAYS VALUES OF KAY,P,T,H

CALL BLOCK(2)

CALL TEXT(F,2,1,1,1HA,F,F)

CALL ENDBLK

BLOCK 3 DISPLAYS A FLASHING * ON THE X-AXIS AT T

CALL BLOCK(3)

CALL TEXT(F,1,100,1,1H*,F,F)

CALL ENDBLK

BLOCK 10 DISPLAYS DATA CURVE AND X-AXIS

CALL BLOCK(10)

CALL TEXT(F,1,1,1,1HA,F,F)

CALL ENDBLK

BLOCK 49 INDICATES THE APPROXIMATION BEING DISPLAYED

CALL BLOCK(49)

CALL TEXT(F,1,1000,20,20HZEROTH APPROXIMATION,TR,F)

CALL ENDBLK

BLOCK 50 DISPLAYS INDICATORS AND INSTRUCTIONS

CALL BLOCK(50)

CALL TEXT(F,-300,-40,47,47H KAY

2 H,TR,F)

CALL TEXT(F,0,0,5,5HCLEAR,TR,F)

CALL TEXT(F,0,-40,4,4HBACK,TR,F)

CALL TEXT(F,0,-80,9,9HHARD COPY,TR,F)

CALL TEXT(F,0,-120,8,8HCONTINUE,TR,F)

CALL TEXT(F,0,-160,12,12HDLINK APPROX,TR,F)

CALL ENDBLK

BLOCK 51 ALLOWS USER TO RESET BLOCK 50 IF IT IS CLEARED

CALL BLOCK(51)

CALL TEXT(F,0,0,5,5HRESET,TR,F)

CALL ENDBLK

BLOCK 52 INDICATES ERROR BY USER

C
CALL BLOCK(52)
CALL TEXT(F,397,512,17,17HERROR - TRY AGAIN,TR,TR)
CALL ENDBLK

C
CALL DISPLY(1,1,0,0)
CALL DISPLY(2,1,0,0)
CALL DISPLY(3,1,0,0)
CALL DISPLY(10,1,0,0)
CALL DISPLY(50,1,810,1000)
CALL DISPLY(51,1,810,1000)
CALL DISPLY(52,1,0,0)
CALL ERSBK(51)
CALL ERSBK(52)
RETURN
END

MEMORY REQUIREMENTS 00059A BYTES


```
SUBROUTINE GRID(II,TI,KAY,KAYN,V,T,OP,P,PN,JN,NPERD,HERE,XSCALE,
2*,*,*,*)
```

```

C
C SUBROUTINE GRID DECIDES AND PERFORMS
C INSTRUCTIONS FROM THE GRID USER
C
C INTEGER*2 AX(100),AY(100),STRING(10)
C INTEGER BLK(3),STATUS,KEY
C REAL KAY,TI,T(100),V(100)
C LOGICAL*1 ON,ERR,F/.FALSE./,TF/.TRUE./,FLASH/.FALSE./
C
C APPROXIMATION CURVE IS DISPLAYED
C
C WRITE(6,103) II
103 FORMAT(15H APPROXIMATION ,II,14H NOW DISPLAYED)
C III = II + 1
C CALL DISPLY(49,1,0,0)
C DO 5 I = 1,NPERD
C SCIENT = T(I)/XSCALE
C AX(I) = ALOG10(SCIENT)*200
5 AY(I)=V(I)*1000
6 CALL DELBLK(1)
C CALL BLOCK(1)
C CALL DLINE(F,F,AX,AY,NPERD,FLASH,F)
C CALL ENDBLK
C CALL DISPLY(1,1,0,HERE)
C
C CONTROL TRANSFERRED TO GRID USER
10 CALL TRANMT
C
C ERROR INDICATION ERASED IF NECESSARY
C CALL ERSEK(52)
C
C GO TO 200 IF LIGHT PEN USED
C CALL OLPEN(1,IX,IY,ITYPE,IO,BLK,&100)
C
C GO TO 500 IF KEYBOARD . . . OTHERWISE DO FOR
C CALL DALPHA(1,IX,IY,NUM,10,STRING,&500)
9 CALL PSTBK(52)
C GO TO 10
C
C LIGHT PEN
C
C GO TO 300 IF USER HAS PICKED A POINT ON THE GRAPH
C . . . THAT IS, WISHES TO CHANGE T
200 IF(IX.LT.810) GO TO 300
C
C CLEAR OR RESET INSTRUCTIONS
C IF(IY.GT.980) GO TO 210
C
C GO BACK TO PREVIOUS APPROXIMATION OR DATA CURVE
C IF(IY.GT.940) RETURN1
C
C HARD COPY
C IF(IY.GT.900) GO TO 240

```



```

C
C   CONTINUE TO NEXT APPROXIMATION
C   IF(IY.GT.400) GO TO 250
C
C   FLASH APPROXIMATION CURVE
C   IF(IY.GT.220) GO TO 260
C
C   OTHERWISE ERROR
C   GO TO 9
C
C   <<<<<>>>><<<<<>>>><<<<<>>>><<<<<>>>><<<<<>>>><<<<<>>>>
C
C
C   CLEAR/RESET
C
210 IF(UN) GO TO 215
    CALL ERSBK(51)
    CALL RSTBK(50)
    CALL PSTBK(2)
    CN = .TRUE.
    GO TO 10
215 CALL ERSBK(50)
    CALL RSTBK(51)
    CALL ERSBK(2)
    DN = .FALSE.
    GO TO 10
C
C   HARD COPY
C
240 CALL ERSBK(50)
    CALL ERSBK(2)
    CALL SNAP(0.015)
    CALL RSTBK(50)
    CALL RSTBK(2)
    GO TO 10
C
C   CONTINUE
C
250 CALL DALPHA(2,IX,IY,NUM,10,STRING,&250)
    GO TO 9
C   KEY FOR NEXT APPROXIMATION MUST HAVE BEEN ENTERED
C   AT GRID KEYBOARD
255 CALL KR(KAYN,R,RN,STRING,NUM,II+1,III+1,&9)
    RETURN4
C
C   MAKE THE APPROXIMATION CURVE BLINK OR STOP BLINKING
C
260 FLASH = .NOT.FLASH
    GO TO 6
C
C   NEW VALUE FOR T
C
C   CHECK IF USER HAS TYPED IN A VALUE FOR T . . .
300 CALL DALPHA(2,IX,IY,NUM,11,STRING,&350)
C   . . . IF NOT, THEN USE POSITION OF LIGHT PEN

```



```
360 TI = XSCALE*10**(IX/200.)  
RETURN3
```

```
C      . . . IF SC, THEN CONVERT AND USE VALUE FROM GRID KEYBOARD
```

```
350 IF(0.EQ.MOD(NUM,2)) NUM = 2*NUM  
    IF(1.EQ.MOD(NUM,2)) NUM = 2*NUM-1  
    TI = CHRFLT(STRING,NUM,ERR)  
    IF(ERP) GO TO 9  
RETURN3
```

```
C
```

```
C      KAY ENTERED AT KEYBOARD
```

```
C
```

```
500 CALL KR(KAY,RP,R,STRING,NUM,II,III,&9)  
RETURN?  
END
```

MEMORY REQUIREMENTS 000002 BYTES

SUBROUTINE KR(KAY,RP,R,STRING,NUM,II,III,*)

C
C KR DECODES KAY,CALCULATES R AND DISPLAYS THEIR VALUES
C

LOGICAL*1 TR/.TRUE./,F/.FALSE./,ERR

INTEGER*2 STRING(10)

REAL KAY,R

NUM = 2*NUM - MOD(NUM,2)

500 KAY = CHRFLT(STRING,NUM,ERR)

IF(ERR) RETURN

FRAC = (1.0 - KAY)/(1.0 + KAY)

P = RP/FRAC**2

WRITE(6,102) II,KAY,III,R

102 FORMAT(4F KAY,II,3H = ,F10.3,10X,3H R(,II,4H) = ,F10.3)

CALL DELBLK(2)

CALL BLOCK(2)

CALL TEXT(F,1,930,8,STRING,TR,F)

CALL FITCHR(R,STRING,8,2)

CALL TEXT(F,192,930,8,STRING,TR,F)

CALL ENDBLK

CALL DISPLY(2,1,0,0)

RETURN

END

MEMORY REQUIREMENTS 00038A BYTES

SUBROUTINE TH(T,H,IFFR,XSCALE)

C
C TH DISPLAYS T AND H AND FLASHING * AT T ON THE X-AXIS
C

LOGICAL*1 TR/.TRUE./,F/.FALSE./
INTEGER*2 STRING(15)
CALL DELBLK(2)
CALL BLOCK(2)
CALL FLTCHR(T,STRING,9,2)
CALL TEXT(F,416,930,9,STRING,TR,F)
CALL FLTCHR(H,STRING,8,2)
CALL TEXT(F,672,930,8,STRING,TR,F)
CALL ENDBLK
CALL DISPLY(2,1,0,0)
CALL DELBLK(3)
CALL BLOCK(3)

ITX = 200 * ALOG10(T/XSCALE)
CALL TEXT(F,ITX,0,1,1H*,TR,TR)
CALL ENDBLK
CALL DISPLY(3,1,0,INFR)
RETURN
END

MEMORY REQUIREMENTS 000318 BYTES
36.115 PC=0

B29997